

# **Short-Form Videos and Mental Health: A Knowledge-Guided Multimodal Neural Topic Model**

**Jiaheng Xie**

jxie@udel.edu

Department of Accounting and MIS  
Lerner College of Business & Economics  
University of Delaware

**Ruicheng Liang**

rcliang@mail.hfut.edu.cn

School of Management  
Hefei University of Technology

**Yidong Chai**

chaiyd@hfut.edu.cn

School of Management  
Hefei University of Technology

**Yang Liu**

2039258362@qq.com

School of Management  
Hefei University of Technology

# Short-Form Videos and Mental Health: A Knowledge-Guided Multimodal Neural Topic Model

## ABSTRACT

While short-form videos head to reshape the entire social media landscape, experts are exceedingly worried about their depressive impacts on viewers, as evidenced by medical studies. To prevent widespread consequences, platforms are eager to predict these videos' impact on viewers' mental health. Subsequently, they can take intervention measures, such as revising recommendation algorithms and displaying viewer discretion. Nevertheless, applicable predictive methods lack relevance to well-established medical knowledge, which outlines clinically proven external and environmental factors of depression. To account for such medical knowledge, we resort to an emergent methodological discipline, seeded Neural Topic Models (NTMs). However, existing seeded NTMs suffer from the limitations of single-origin topics, unknown topic sources, unclear seed supervision, and suboptimal convergence. To address those challenges, we develop a novel Knowledge-guided Multimodal NTM to predict a short-form video's depressive impact on viewers. Extensive empirical analyses using TikTok and Douyin datasets prove that our method outperforms state-of-the-art benchmarks. Our method also discovers medically relevant topics from videos that are linked to depressive impact. We contribute to IS with a novel video analytics method that is generalizable to other video classification problems. Practically, our method can help platforms understand videos' mental impacts, thus adjusting recommendations and video topic disclosure.

**Keywords:** short-form video, depressive impact, neural topic model, design science, prediction.

# **Short-Form Videos and Mental Health: A Knowledge-Guided Multimodal Neural Topic Model**

## **INTRODUCTION**

Short-form video platforms, such as TikTok, Reels, and Douyin, have drastically transformed netizens' content consumption behaviors online in recent years. TikTok, in particular, has surpassed Google and Facebook as the world's leading Web domain (Moreno 2021), reaching over 1.5 billion monthly active users and 3 billion downloads in 2023 (Iqbal 2023). While cheering for their success, experts and mainstream media have increasingly warned that short-form video platforms are brewing a dangerous breeding ground for mental disorders (Schlott 2022). Medical studies further endorse such concerns by providing empirical evidence that individuals are more likely to report increased levels of depressive symptoms after using TikTok (Perlis et al. 2021). The reason short-form videos receive overwhelmingly more attention on mental health issues than any other social media forms lies in that the nature of short-form videos is about "*posting very loudly about very intimate and intense things, and people are encouraged to be vulnerable to fit that spirit*" (Paul 2022). In order to curb the uncontrollable influence of short-form videos' impact on viewers' mental health, we aim to predict short-form videos' depressive impact on viewers before they infiltrate the public.

Predicting a short-form video's depressive impact lends multi-faceted practical implications. For short-form video platforms to improve user experience and take on social responsibility, the predicted depressive impact can be accounted for to optimize platforms' recommendation algorithms, such that depressive-impacting videos are not constantly recommended to the same user. Their current recommender systems, however, rely on users' viewing history (Zote 2022), which often bombards depression-prone users with depressive content repeatedly. To comply with any potential regulations on this subject matter, platforms can display viewer discretion on videos

that are predicted to have a depressive impact. The topics in a video's content related to depressive impacts can be included in the viewer discretion to fully inform viewers about potential risks so that they can decide whether to watch the video on their own terms.

A short-form video's depressive impact on viewers can be observed via this video's viewer-generated comments. A comment showing depressive moods indicates that this video has a depressive impact on that viewer at the time of watching. Therefore, we define the depressive impact of a video as the proportion of depressive comments of this video<sup>1</sup>. It is worth noting that highly depressed users are less likely to leave a comment even if a video deteriorates their depressive moods. Nevertheless, the proportion of depressive comments is a conservative measure of a video's depressive impact. That is, if a video's comments already suggest a noticeable depressive impact, its actual depressive impact on the general population should be even higher, which firmly deserves interventions. We will further address this issue by experimenting with various depressive comment proportions<sup>2</sup> as the prediction threshold in the empirical analyses.

The most related literature to this study is social media-based depression prediction. Despite the difference that these studies predict a user's depression status using their social media posts while we focus on the prediction of a video's depressive impact on its viewers, the prediction methods in this area can still offer insights for our methodological development. Existing social

---

<sup>1</sup> We leverage depressive comments to compute the outcome rather than using depression diagnosis because we aim to minimize the depressive impact when users watch short-form videos, which aligns with the concerns of platforms, mainstream media, experts, and parents. Such depressive impacts may contribute to, yet not equivalent to, the depression diagnosis of viewers, which demands interviews at doctors' offices and is often inaccessible for privacy concerns. Understanding depressive impacts of videos already offers fruitful implications for platforms to reduce negative impacts, thus alleviating pressing criticisms from society.

<sup>2</sup> For instance, a video that has depressive impacts on 10% of its actual viewers may correspond to a smaller percentage of depressive comments (e.g., 5%) by the commenters. If the platform can only tolerate depressive impact on up to 10% of its viewers, they can set the prediction threshold at a depressive comment proportion lower than 10% (e.g., 5%). If our method is accurate when the prediction threshold is either 5% or 10% (and many more) of depressive comments, this means our method is effective regardless of whether there is a gap between the proportion of depressive comments and the proportion of actually impacted overall viewers, as platforms can simply set a flexible prediction threshold (depressive comment proportion) that is lower than their target on the general viewers. We will show our models' robustness and accuracy when we define depressive-impacting videos as a variety of depressive comment proportions, including 5%, 10%, 20%, and 30% in Table 9.

media-based depression prediction methods can be broadly categorized into three groups: feature-based machine learning (Li et al. 2019), end-to-end deep learning (Wang et al. 2022), and topic modeling approaches (Tadesse et al. 2019). Feature-based machine learning is not applicable to our study because we are faced with video and audio data, where well-established linguistic features about depression are not obtainable. While end-to-end deep learning outperforms topic models in many tasks, it also faces obstacles compared to topic modeling approaches because the former cannot offer the topics related to video content that led to the prediction result, which is critical information to include in the viewer discretion as discussed above. To elevate the prediction performance of topic models, recent studies incorporate deep learning architectures in topic models, named Neural Topic Models (NTMs). Due to state-of-the-art predictive performance and topic explainability, we build our model upon NTMs.

The topics learned from most NTMs are purely data-driven and lack clinical relevance in the depression setting, where well-established medical ontologies exist that lay out the external and environmental factors of depression. These factors are verified by numerous medical studies to safeguard their accuracy and comprehensiveness. To leverage such medical domain knowledge, it is critical to learn topics related to depression's external and environmental factors in the medical ontology. For instance, watching stories about domestic violence is one such factor, thus increasing viewers' depressive risk (Preidt 2022). This factor can guide the model to detect topics related to domestic violence stories if they appear in a video. Other depressive risk factors can guide the learning of respective topics in the videos as well. An emergent realm of NTMs, named seeded NTMs, is well suited for this goal (Lin et al. 2023). Factors in medical ontologies can serve as the seed words to supervise the learning of topics in NTMs. Despite such great potential, existing seeded NTMs still await modifications to adapt to our context. Firstly, seeded NTMs are mostly developed to learn topics from one origin, while we are faced with videos and comments

that originate from *content creators* and *viewers*, respectively, whose topic generative processes are distinct. Secondly, existing seeded NTMs cannot distinguish whether a learned topic is from the medical knowledge base or newly discovered topics. This information is essential to understand the emerging depressive-impacting content on social media that has not been documented in the medical literature. Thirdly, existing seeded NTMs cannot determine the optimal level of supervision that the seed words should exert for the learning of topics related to the medical knowledge base. Consequently, they cannot determine the best extent to retain the ability to explore other related topics. This is especially critical in the social media context where professional medical ontology could miss out on depressive factors pertaining to the social media environment, such as trending TikTok challenges and recent global crises. Fourthly, the same as extant NTMs, seeded NTMs are often prone to convergence to suboptimal local minimal. This is largely because NTMs need to learn high-dimensional topic-word distributions from the dataset. To address the above limitations, we develop a novel Knowledge-guided Multimodal NTM.

This study makes multiple contributions. Positioned at the intersection of machine learning and its business and societal impact, this study contributes to computational design science research in Information Systems (IS) by designing a novel model to predict the depressive impact of short-form videos. Methodologically, our proposed method extends beyond existing seeded NTMs to address the challenges of single-origin topics, unknown topic sources, unclear seed supervision, and suboptimal convergence. Extensive empirical analyses using real-world short-form video data from two platforms (Douyin and TikTok) demonstrate that our proposed method outperforms state-of-the-art benchmarks. From a practical perspective, short-form video platforms can greatly benefit from our method. They can redesign their video recommendation algorithms to account for the predicted depressive impact of a video. They can also show viewer discretion that discloses the topics in a video related to depressive impacts.

## LITERATURE REVIEW

We review five streams of literature. We first position our work in the social media-based health analytics studies in IS. Following that, we investigate studies on short-form videos and their depressive impacts and explore video-based depression prediction methods. Then, we review depression prediction studies on social media in general and identify opportunities for methodological innovation. Next, we examine seeded neural topic models, as they are related to our work methodologically. Last, we review medical ontology literature as the medical knowledge guide for our model. We conclude this section by highlighting the key novelties of our study compared to the above literature review.

### **Social Media-based Health Analytics Studies in IS**

Health analytics examines patient data and makes diagnostic or prognostic risk predictions (Shmueli and Koppius 2011). It is a critical research area in IS (Shmueli and Koppius 2011), since the research findings have a wide range of societal impacts, such as identifying patients at risk (Bardhan et al. 2015), supporting clinical decision-making (Ben-Assuli and Padman 2020), and dealing with hospital administrative challenges (Meyer et al. 2014). Our study falls into the domain of health predictive analytics in IS: we seek to address the difficulties of accurate depressive impact prediction of short-form videos using multimodal social media data.

Social media data have significant potential and implications for addressing socio-technical concerns. Leveraging such data becomes an emerging and vital research avenue in IS (Hedman et al. 2013). IS researchers have used social media data to generate new IT artifacts to address healthcare challenges. For example, Zhang and Ram (2020) extract digital traces from social media, environmental sensors, and health records to identify asthma risk factors. Xie et al. (2022) retrieve social media data to discover reasons for medication nonadherence. While academics have suggested that unique social media data coupled with domain knowledge and appropriate

analytics methods can serve as the foundation for a “21<sup>st</sup>-century science” (Hedman et al. 2013), they have also pointed out that IS researchers could reap benefits from emergent skills and tools to leverage these data and exploit them effectively (Hedman et al. 2013). Our work aligns with this research direction: we intend to design a new IT artifact that leverages a medical knowledge base to decipher short-form video data and predict short-form videos’ depressive impacts.

### **Short-form Videos and Depressive Impacts**

As short-form video platforms, such as TikTok, Reels, and Douyin, gain soaring popularity amongst the younger generation, their impact on viewers’ mental health (e.g., depressive moods) has increasingly become an alarming concern for society. Consequently, mainstream media has been calling for policymakers to enact stricter regulations and academics to investigate short-form videos’ impact on viewers’ depressive moods (Paul 2022). Echoing those concerns, extant studies in this area employ surveys and interviews to understand viewers’ perceptions and behavior change after using short-form video apps (Milton et al. 2023; Zahra et al. 2022). Zahra et al. (2022), Milton et al. (2023), and Carpenter (2023) establish empirical evidence of short-form videos’ association with viewers’ depressive moods, most likely arising from the “For You” page. Zhang et al. (2022) and Chao et al. (2023) attempt to understand the factors that cause depressive impacts on viewers, including physical activity, sleep quality, and psychosocial factors, among others. Due to the recency of this issue, predictive analytics studies in this area are yet to emerge, despite their pivotal role in suppressing large-scale mental influence on viewers. Witnessing this timely opportunity, this study aims to predict a short-form video’s depressive impact on viewers before it causes widespread influence.

The closely related paradigm to our goal is the video-based depression prediction literature. These studies take a video of a participant as the input to predict his or her depression status. These videos are usually collected from clinical interviews (e.g., DAIC-WoZ dataset and AViD-

Corpus), where participants' facial expressions and spoken language are indicative of their depression status (He et al. 2021; Lin et al. 2020; Toto et al. 2021). The common methods deployed in this area include machine learning methods, such as Support Vector Machine (SVM) (Yang et al. 2017) and Decision Trees (DT) (Yang et al. 2016), and deep learning methods, such as Convolutional Neural Network (CNN) (He et al. 2021) and Bidirectional Long Short-Term Memory (Bi-LSTM) (Lin et al. 2020; Toto et al. 2021).

Yet both aiming to leverage video data to combat mental health issues, our study is largely distinct from video-based depression prediction studies from the perspectives of problem formulation and datasets. In terms of problem formulation, prior studies use a video of a user to predict this user's current depression status, where a user is the prediction unit. The practical implication for them resolves around suggesting treatment resources to the target user. Our study, on the other hand, focuses on leveraging a short-form video on social media to forecast its depressive impact on its viewers, where a video is the prediction unit. Our practical implication centers around minimizing short-form videos' depressive impact on the platforms' end. For instance, our work can be integrated into the design of video recommendation algorithms that currently rely on users' viewing history (Zote 2022). Knowing each video's potential depressive impact, new recommender systems can make sure the same user is not constantly recommended depressive-impacting videos, even if this user has watched them in the past. Turning to datasets, video-based depression prediction studies mostly use clinically recorded videos of a patient to predict their depression status, where the useful information is users' facial expressions and language. Our study is positioned in the short-form video context, where the videos are shared on social media platforms and are not related to viewers' physiological cues. The information in the video related to its depressive impact on viewers is linked to the topics, visual presentations, and acoustic effects. To understand depression prediction methods developed in the social media

context, we further review depression prediction studies on social media.

### **Depression Prediction on Social Media**

Three main categories of methods exist in social media-based depression prediction: feature-based machine learning, end-to-end deep learning, and topic modeling. Feature-based machine learning studies are interested in crafting textual features (Li et al. 2019), guided by theories of depression (Zulkarnain et al. 2020). For example, due to self-awareness and reduced social connections, the frequent use of first-person singular words, such as “I,” are often used to detect depression (Bucur et al. 2021). Previous studies have also found that frequent use of negative emotional words and absolutist words is common among depressed patients (Li et al. 2019). These linguistic features can be captured by Linguistic Inquiry and Word Count (LIWC) and Part of Speech (POS) techniques (Bucur et al. 2021; Pennebaker et al. 2001). Beyond the linguistic features, a few studies design domain-specific features, such as antidepressant word count per post (Zulkarnain et al. 2020). In addition to textual data, other studies extract features from other data modalities, such as images and posting time (Liu et al. 2022).

End-to-end deep learning studies in this area directly take the original social media post as the input and yield users’ depression status. As depressed patients often use informal and implicit words to express their emotions, embedding techniques are used to capture accurate and rich semantics (Pérez et al. 2022). Given that depressed patients have a sequence of posts, LSTMs have become essential components in capturing the evolution of patients’ moods and symptoms over time (Ghosh and Anwar 2021). A few studies have also utilized CNNs to process textual data to extract local features, such as depression-related phrases, as well as global features for depression prediction (Wang et al. 2022). To enhance the model’s predictive power by capturing important clues related to depression, depression prediction methods with attention mechanisms such as Hierarchical Attention Network (HAN) have been proposed (Cheng and Chen 2022).

Topic modeling approaches for depression prediction usually design Latent Dirichlet Allocation (LDA)-based methods to discover topics in social media posts. For instance, Tadesse et al. (2019) use LDA to extract topics that serve as features for an SVM classification model. Yazdavar et al. (2017) design a semi-supervised topic model based on LDA to monitor depression symptoms. Guo et al. (2023) develop a prompt-based topic model for depression prediction on data sources with few labels.

While the above three categories of studies and our study are all positioned in the social media and mental health context, our study is significantly different from social media-based depression prediction studies. Similar to video-based depression prediction studies, social media-based depression prediction studies focus on the prediction of *a user*'s depression status, either based on a user's single post (also known as the post-level prediction) or a user's series of historical posts (also known as the user-level prediction). Their implications pertain to sending treatment information and educational resources to depressed users. Nevertheless, our study targets a different lens and aims to make a prediction of *a video*'s depressive impact on viewers whose implications focus on the intervention measures on the platforms' end (e.g., recommender system modification and viewer discretion) to minimize such an impact. Apart from that, depression prediction studies on social media mostly center around textual data, such as Twitter and Reddit. Multimodal video data on emergent short-form video platforms are rarely attended.

While our study has differences from social media-based depression prediction studies, their methods can still shed light on our method design. Feature-based machine learning methods are not directly applicable to our study because those features are more suited for textual data, while we are faced with video and audio data. Besides, manually engineered features have to be pre-defined, which requires expensive domain expertise. Crafting those features also relies on human judgments, which are independent of the learning objective of the depression classification

model. Separating the feature learning and classification model may result in suboptimal prediction performances. End-to-end deep learning models overcome such a limitation by learning the features jointly with the classification model. However, deep learning models are not able to explain what the learned features mean in a practical sense. Topic model-based approaches are explainable in the sense that the learned topics can semantically indicate why a video is classified as having a depressive impact. Such topic-based explanation is useful to short-form video platforms for regulatory compliance considerations. When our model predicts a video is likely to have a depressive impact on viewers, on one hand, platforms can factor in such information in the video recommendation algorithm. On the other hand, however, the platform cannot remove a video sorely because it may cause a depressive impact to avoid the violation of the Freedom of Speech. The learned topics can alleviate this issue. Short-form video platforms can display viewer discretion informing the inferred topics in the video that might induce depressive moods. The viewers can decide at their own discretion whether to continue watching the video. To facilitate such topic-based viewer discretion and explanation, we follow the topic modeling approach to design our method. Although topic models are naturally suited for the short-form video context, their predictive power is shy of deep learning models. Fortunately, an emergent stream of research, neural topic models, has been integrating deep learning into topic models to harness state-of-the-art predictive power as well as topic interpretability.

### **Seeded Neural Topic Model**

Topic modeling techniques have the benefit of modeling words and documents uniformly under a probabilistic framework. However, they also suffer from restrictive assumptions and inference efficiency problems, which can be remedied by deep learning techniques (Cao et al. 2015). Born at the intersection of topic modeling and deep learning architectures, Neural Topic Models (NTMs) have successfully boosted the performance, efficiency, and usability of topic modeling

(Zhao et al. 2021). NTMs can be broadly categorized into four groups (Zhao et al. 2021). The first group, representing the vast majority of NTMs, leverages Variational Autoencoders (VAEs) and Amortized Variational Inference (AVI) to extend the generative process and amortize the inference process of topic models (Srivastava and Sutton 2016; Zhang et al. 2018). An encoder is used to learn the representation of the input text (or videos and audios in our study). A decoder is then added to generate word distributions (topics), which can further predict the given task. The encoder, decoder, and classification are learned in an end-to-end manner. Therefore, the learned topics can inherently interpret what contributes to the prediction result. The second group proposes autoregressive NTMs, where the predictive probability of a word in a document is conditioned on its hidden state, which is further conditioned on the previous words (Gupta et al. 2019). The third group adapts the Generative Adversarial Networks (GANs) for topic modeling. Wang et al. (2019) propose a GAN generator that takes a random sample of a Dirichlet distribution as a topic distribution and generates the word distributions of a “fake” document conditioning on the topic distribution. A discriminator is introduced to distinguish between generated word distributions and real word distributions obtained by normalizing the TF-IDF vectors of real documents. The fourth group considers the graph presentations of a corpus of documents and uses a variety of Graph Neural Networks (GNNs) to discover latent topics (Zhu et al. 2018). The latter three groups are more suited to textual data, as they necessitate conditional word distributions or graph structure of words, which are not applicable to our study. As a result, we build our model upon the most widely recognized VAE-based NTMs.

Although NTMs have demonstrated exciting performances in various tasks, their topics are typically learned with the purpose of minimizing the loss function of the given task on the actual dataset. Consequently, the semantics and quality of the learned topics may not offer clear and domain-relevant interpretable insights for domain experts and end users. This is especially true

for health analytics studies, where the medical knowledge base lends a solid foundation about the potential risk factors that can explain a health outcome. In order to “teach” the NTMs to learn topics that are relevant to a target knowledge base and simultaneously maximize the prediction accuracy, recent studies have proposed seeded NTMs, where seed words are selected from the knowledge base to supervise the learning of topics. The learned topics can be interpreted according to the knowledge base while still maintaining the capability of discovering other yet similar topics (Lin et al. 2023). For instance, Lin et al. (2023) propose the SeededNTM with a context-dependency assumption to alleviate the ambiguities with context document information and an auto-adaptation mechanism to automatically balance between multi-level information. Cheng et al. (2023) develop the SBERT NTM that includes an Easy Data Augmentation (EDA) method with keyword combination to overcome the sparsity problem in short texts. Fard et al. (2020) design a seed-guided deep document clustering approach that jointly learns deep representations and biases the clustering results through the seed words.

The seeded NTMs are especially relevant to our study because carefully designed seed words can provide effective directional guidance to interpret the prediction of a video’s depressive impact. Faithfully designing the seed words in our context is well supported by the widely established medical knowledge about the external and environmental factors of depression, known as medical ontologies. Those risk factors can function as the seed words to supervise the learning of topics in the NTM. Thanks to the rigorous validation of the risk factors established in the medical literature, they could not only improve the prediction performance of our model but also safeguard the clinical relevance of our topic interpretability.

The existing seeded NTMs still fall short in our context. Firstly, most existing seeded NTMs focus on one origin of data, such as posts from *the users*. However, we are faced with videos and comments from different origins. On one hand, video topics are generated by *content creators*.

On the other hand, comments generated by *viewers* can be fruitfully utilized in the model *training phase* (not the test or prediction phases) to understand the perception of the *viewers*, as our goal is to predict the depressive impact on *viewers*. Content creator-generated content and viewer-generated content are distinct in terms of topics, thinking processes, and personalities. A single-origin topic generative process is insufficient to capture such nuances between content creators and viewers. Secondly, once the topics are learned by existing seeded NTMs, it is unclear about the probability of a topic originating either from the given knowledge base or from newly discovered topics. This information is especially critical in our context because if a new topic contributing to depressive impacts is discovered on social media, it can complement the existing medical knowledge that is geared toward formal medical risk factors, whereas factors on social media relate more toward personal experience, trending social media challenges, and recent global events. The understanding of such trending factors helps therapists and psychiatrists be more relatable to patients and gain a holistic view of both professional depression diagnosis factors and personal and emerging events contributing to depressive moods. Thirdly, existing seeded NTMs typically use distance measures (e.g., Kullback-Leibler divergence) to constrain the learned topics in the learning process. The weight of such a constraint needs to be manually defined and fine-tuned. Overweighting such a constraint would limit the model's capability to discover other similar topics. Underweighting such a constraint would diminish the supervising role of the seed words. Fourthly, the same as most NTMs, the existing seeded NTMs randomly initialize topic-word distributions and learn them from scratch. A topic-word distribution is a matrix whose number of rows is equivalent to the number of distinct words. The high dimensionality of the output distribution causes the learning process to converge to suboptimal local minimal, hurting prediction performances and generalizability.

## **Medical Ontology**

To understand the medical knowledge to serve as the seed words for NTMs in our study, we refer to the medical ontology literature. Ontology is the science of what is, including the types and structures of objects, properties, events, processes, and relationships (Smith 2003). Ontology is widely used in computer and information science to provide a standard vocabulary for researchers to share information. It provides machine-interpretable definitions of fundamental concepts of the domain and relations between the concepts (Smith 2003). In medical expert systems, ontology has been used to represent medical domain knowledge for disease risk factors (Arsene et al. 2011; Zheng et al. 2007). For depression analytics studies, ontology-based approaches have been used to represent factors related to depression (Chang et al. 2013; Jung et al. 2017).

Given the unique context of each study, research findings from multiple relevant medical studies can be ensembled to construct the most appropriate knowledge base (ontology), provided that the constructed ontology is evaluated by domain experts. In the social media context, the following three aspects from videos could have a depressive impact on viewers and are often shared as narratives or visual presentations: (1) Sharing depressive symptom experiences, such as anxiety, fatigue, low mood, reduced self-esteem, change in appetite or sleep, suicide attempt, and more (APA 2022; Beck and Alford 2009; Martin et al. 2006; Rush et al. 2003). Video contents related to these symptom experiences have a contaminating effect on viewers. (2) Sharing major life event stories, such as divorce, body shape, violence, abuse, drug or alcohol use, and so on (Beck and Alford 2009). These stories are usually traumatizing, which causes viewers to cast doubts about their own lives and relationships as well. (3) Sharing ongoing treatment experiences (Beck and Alford 2009). These experiences are often unpleasant for those who share on social media. Watching those contents is likely to induce depressive moods in viewers. Following this medical literature, we adopt this three-component ontology as the knowledge base to guide our model design. In the empirical analysis, we will further evaluate this constructed ontology

quantitatively and validate it with medical experts. To clarify, these depression's external and environmental factors are the most salient ones documented in the medical literature. They are by no means an exclusive set of factors, especially in the actively evolving social media space. This motivates us to design our model to retain the ability to learn new depressive-impacting factors.

### **Key Novelties of Our Study**

From the problem formulation perspective, our study focuses on the prediction of the *depressive impact of a video* on its viewers. This sets us apart from the existing social media-based depression prediction studies that predict the *depression status of a user*. As mentioned above, the implications of these two streams of studies drastically differ. From the method perspective, our proposed method extends beyond existing seeded NTMs in four aspects. Firstly, to account for the different thinking processes of content creators and viewers, we design two distinct generative processes for videos and comments. Secondly, to tackle the issue of not knowing the probability of the topic learned either from the existing knowledge base or from the trending social media context, we learn two sets of topics: seed topics and regular topics. Seed topics reflect well-established medical knowledge, while regular topics relate to new topics, such as trending events. The probability of either set of topics reflects the degree of the topics coming from the existing knowledge base or from the trending social media context. Thirdly, to address the challenge of manual definition and tuning of the constraint of seed words, the level of supervision from the seed words is data-driven and can be reflected as the probability of a topic coming from either the existing knowledge base or social media context. We design a Beta prior for such a probability and learn a posterior for it to automatically determine the appropriate probability value, i.e., the approximate level of knowledge supervision. Fourthly, to resolve the problem of convergence to suboptimal local minimal of NTMs, we pre-train a regular and seed topic-word distribution and design a prior based on a LogNormal distribution. The randomness involved in the generative

process also makes it incompatible with deep learning architectures. We subsequently derive a transformed generative process that retains the advantages of the original generative process and seamlessly works with deep learning architectures as well.

## THE PROPOSED KNOWLEDGE-GUIDED MULTIMODAL NEURAL TOPIC MODEL

### Problem Formulation

A video is inherently a multimodal data format, encompassing transcripts, images, motions, and audios. Among them, transcripts carry the most semantic meaning and deliver human-perceivable content that can be depressive-impacting. Common depressive risk factors are conveyed via transcripts as well. Persuasive and inciting images, motions, and audios further resonate a vulnerable mental state that stimulates such a depressive-impacting scenario. The number of distinct words in the transcripts and comments is denoted as  $V$ . The number of topics in the transcripts is denoted as  $K$ , where the  $k$ -th topic is a  $V$ -dimensional vector whose  $v$ -th element is the probability of the  $v$ -th word. These topics are guided by medical knowledge by setting the seed words as the depressive impact risk factors documented in the depression ontology. Our model still retains the ability to discover other topics. A word with a high probability indicates that this word is highly related to the corresponding topic. As a video usually conveys certain topics, words with a high likelihood of appearing typically display significant semantic correlations with those topics. Those words are called the top words of the topic.

Given a video  $d$  from a set of  $D$  videos, we denote its transcript as  $\tilde{\mathbf{w}}_d$ , which is a list of words denoted as  $[\tilde{w}_{d,1}, \tilde{w}_{d,2}, \dots, \tilde{w}_{d,\tilde{N}_d}]$ . This video's images, motions, and audio modalities are processed and vectorized by deep learning models, and the resulting feature representations are denoted as  $\mathbf{f}_d^I$ ,  $\mathbf{f}_d^M$ , and  $\mathbf{f}_d^A$ . Our Knowledge-guided Multimodal NTM can identify topics from *these four data modalities jointly*. The overall topic distribution of a multimodal video is a vector whose  $k$ -th dimension represents the probability of the  $k$ -th topic. As each topic carries a specific

semantic meaning, its probability reflects the proportion of different contents in the video.

The objective of this study is to automatically discover depressive-impacting topics contained in a given video and subsequently predict this video's likelihood of inducing a depressive impact. A portion of short-form videos do not have narratives, and thus cannot generate transcripts. We design a topic inference model to accommodate those videos. Formally, for a new video  $d$ , we first aim to extract its topic (denoted as  $\boldsymbol{\theta}_d$ ) *from all data modalities*, i.e.,  $\boldsymbol{\theta}_d \leftarrow \text{InferTopic}(I[\tilde{\mathbf{w}}_d], \mathbf{f}_d^I, \mathbf{f}_d^M, \mathbf{f}_d^A)$ , where  $I[\cdot]$  is an indicator function of whether the video contains transcript or not. Then, we aim to predict the label of the depressive impact of a video based on  $\boldsymbol{\theta}_d$ , i.e.,  $y_d \leftarrow \text{PredictLabel}(\boldsymbol{\theta}_d)$ .

The topic inference model and the label prediction model are learned from the training set, where each video contains comments written by viewers and the corresponding label. Those comments are reflective of the viewers' perspective on videos' content and thus can assist the learning of the InferTopic and PredictLabel models to better predict videos' depressive impact on viewers. It is worth noting that, in the test set and new prediction cases, we do not rely on comments. Formally, we denote the comments of video  $d$  as  $\mathbf{w}_d$ , which is also a list of words denoted as  $[w_{d,1}, w_{d,2}, \dots, w_{d,N_d}]$ . Then, we train the InferTopic and the PredictLabel models on the training set, i.e.,  $(\text{InferTopic}, \text{PredictLabel}) \leftarrow \text{Train}(\tilde{\mathbf{W}}, \mathbf{W}, \mathbf{F}^I, \mathbf{F}^M, \mathbf{F}^A, \mathbf{Y})$ , where  $\tilde{\mathbf{W}}$  is the collection of  $\tilde{\mathbf{w}}_d$  of all videos in the training set. Similar notations apply to  $\mathbf{W}, \mathbf{F}^I, \mathbf{F}^M, \mathbf{F}^A$ , and  $\mathbf{Y}$ .

In what follows, we first describe our proposed generative process that addresses the technical challenges. We then identify its incompatibility with our deep learning architecture, which motivates us to devise the transformed generative process. Next, we articulate the variational inference method for the transformed generative process. In the end, we discuss how to utilize the learned topics to predict videos' depressive impacts.

## The Generative Process

In line with topic model-based studies, we design the generative process to model how video data are generated. This generative process allows us to discover the topics and predict the depressive impact of a new video. In this paper, the superscript R refers to notations related to regular topics (discovered from social media context), and the superscript S refers to notations related to seed topics (related to medical knowledge base). The “~” hat symbol refers to transcript-related notations, and the notations without the “~” hat symbol refer to those about all data modalities.

As videos are generated by *content creators* while the comments are generated by *viewers*, their expression patterns, personalities, and thinking processes are usually different. To accommodate such distinctions of origins, we design two sets of generative processes, one for videos and one for comments. For each video  $d$ , we denote its topic from all data modalities as  $\boldsymbol{\theta}_d$ . As each element of  $\boldsymbol{\theta}_d$  is non-negative and they sum up to 1, we first generate an auxiliary variable  $\mathbf{r}_d$  from a normal distribution and then transform it with softmax. This is a common practice in NTMs (Chai et al. 2024). We denote the topic from its transcript as  $\tilde{\boldsymbol{\theta}}_d$ . As transcripts are one of the modalities of videos, the corresponding topic  $\tilde{\boldsymbol{\theta}}_d$  should be a subset of  $\boldsymbol{\theta}_d$ . We draw  $\tilde{\boldsymbol{\theta}}_d$  from  $\boldsymbol{\theta}_d$  with multiple Bernoulli distributions, each of which is for one topic. The mean of each Bernoulli distribution is the probability of each topic to be drawn (remained), computed as  $\mathbf{h}_d = \beta \cdot \boldsymbol{\theta}_d$ , where  $\beta$  is the ratio of the number of transcript topics over the number of video topics. We use the indicator  $\mathbf{I}_d$  whose  $k$ -th element equals 1 if topic  $k$  is remained, and equals 0 if otherwise. Hence,  $\boldsymbol{\theta}_d \circ \mathbf{I}_d$  represents the remaining topics, where  $\circ$  is the Hadamard product. We then normalize  $\boldsymbol{\theta}_d \circ \mathbf{I}_d$  to make sure the sum of the elements in the topic equals 1. For instance, assuming the video topics  $\boldsymbol{\theta}_d = [0.2, 0.3, 0.5]$  and  $\beta = 0.6$ . We further assume, from three Bernoulli distributions, we obtain  $\mathbf{I}_d = [1, 0, 1]$ , which means only the first and the third topics

remain in the transcript. Hence,  $\boldsymbol{\theta}_d \circ \mathbf{I}_d = [0.2, 0, 0.5]$ . The normalized one (i.e.,  $\tilde{\boldsymbol{\theta}}_d$ ) becomes  $[2/7, 0, 5/7]$ . As  $\mathbf{h}_a = \beta \cdot \boldsymbol{\theta}_d$ , normalizing  $\boldsymbol{\theta}_d \circ \mathbf{I}_d$  is the same as normalizing  $\mathbf{h}_d \circ \mathbf{I}_d$ . Hence, we can just use  $\mathbf{h}_d$  and  $\mathbf{I}_d$  to generate  $\tilde{\boldsymbol{\theta}}_d$  without  $\boldsymbol{\theta}_d$ . The generated  $\tilde{\boldsymbol{\theta}}_d$  is then used to generate each word  $\tilde{w}_i$  in the transcript, which is similar to that in the traditional seeded LDA (Card et al. 2018). For images, motions, and audios, as  $\mathbf{f}_d^I$ ,  $\mathbf{f}_d^M$ , and  $\mathbf{f}_d^A$  are intricate, we use neural networks to generate them based on video topic  $\boldsymbol{\theta}_d$ . Neural networks can learn to highlight the critical part of  $\boldsymbol{\theta}_d$  in generating different representations. The architectural details of these neural networks are shown in Appendix 1. For the second generative process (i.e., the one proposed for comments), as comments are generated after viewers perceive all data modalities, the topics should be the same as the video’s topic  $\boldsymbol{\theta}_d$ . Each word of the comments is then generated based on  $\boldsymbol{\theta}_d$ , with a similar process to transcripts. However, we introduce two sets of regular topic-word distributions, denoted as  $\tilde{\boldsymbol{\phi}}^R$  and  $\boldsymbol{\phi}^R$  to account for the distinction between content creators and viewers. Both  $\tilde{\boldsymbol{\phi}}^R$  and  $\boldsymbol{\phi}^R$  are matrices whose  $k$ -th rows are the probability of each word in topic  $k$ , denoted as  $\tilde{\boldsymbol{\phi}}_k^R$  and  $\boldsymbol{\phi}_k^R$ , respectively. Each word  $\tilde{w}_i$  of the transcripts is generated by  $\tilde{\boldsymbol{\phi}}^R$ , while each word  $w_i$  of the comments is generated by  $\boldsymbol{\phi}^R$ . As video modalities and comments are generated based on different processes, we address the problem of single origin.

We denote the  $k$ -th seed topic as  $\boldsymbol{\phi}_k^S$ , which is a  $U$ -dimensional vector indicating the distribution of each seed word, where  $U$  is the number of seed words. The seed words represent the medical knowledge from the depression ontology. We introduce two indicator variables  $\tilde{x}_i$  and  $x_i$  to denote whether the corresponding words  $\tilde{w}_i$  and  $w_i$  are from the existing knowledge base (i.e.,  $\boldsymbol{\phi}^S$ ) or from trending social media context (i.e.,  $\tilde{\boldsymbol{\phi}}^R$  or  $\boldsymbol{\phi}^R$ ). As  $\tilde{x}_i$  and  $x_i$  are binary, we introduce Bernoulli distributions for them. We further assume in different topics, the probability that a word comes from the social media context varies. Hence, we assume the probability that a

transcript word  $\tilde{w}_i$  of topic  $k$  comes from the regular topic is  $\tilde{\pi}_k$  and that the probability from the seed topic is  $1 - \tilde{\pi}_k$ . Hence,  $\tilde{\pi}_k$  reflects the degree of topic  $k$  coming from the trending social media context, while  $1 - \tilde{\pi}_k$  reflects the degree of topic  $k$  coming from the existing knowledge base, thereby addressing the issue of unknown topic sources.

As the words of topic  $k$  are generated either from the seed topic  $\phi_k^S$  or from the regular topics  $\tilde{\phi}_k^R$  and  $\phi_k^R$ , both  $\tilde{\phi}_k^R$  and  $\phi_k^R$  are encouraged to be consistent with  $\phi_k^S$  to increase the likelihood in the learning phase. Therefore, the regular topics are supervised by medical knowledge via seed words. The level of supervision is controlled by  $\tilde{\pi}_k$  and  $\pi_k$ , which are learned from the data. We further introduce Beta distributions as the prior for  $\tilde{\pi}_k$  and  $\pi_k$  and obtain the posteriors for them, which helps to learn  $\tilde{\pi}_k$  and  $\pi_k$  more effectively. As a result, the probability of a topic coming from either the existing medical knowledge or social media context can be attained. Meanwhile, the supervision from seed words is data-driven without manual efforts.

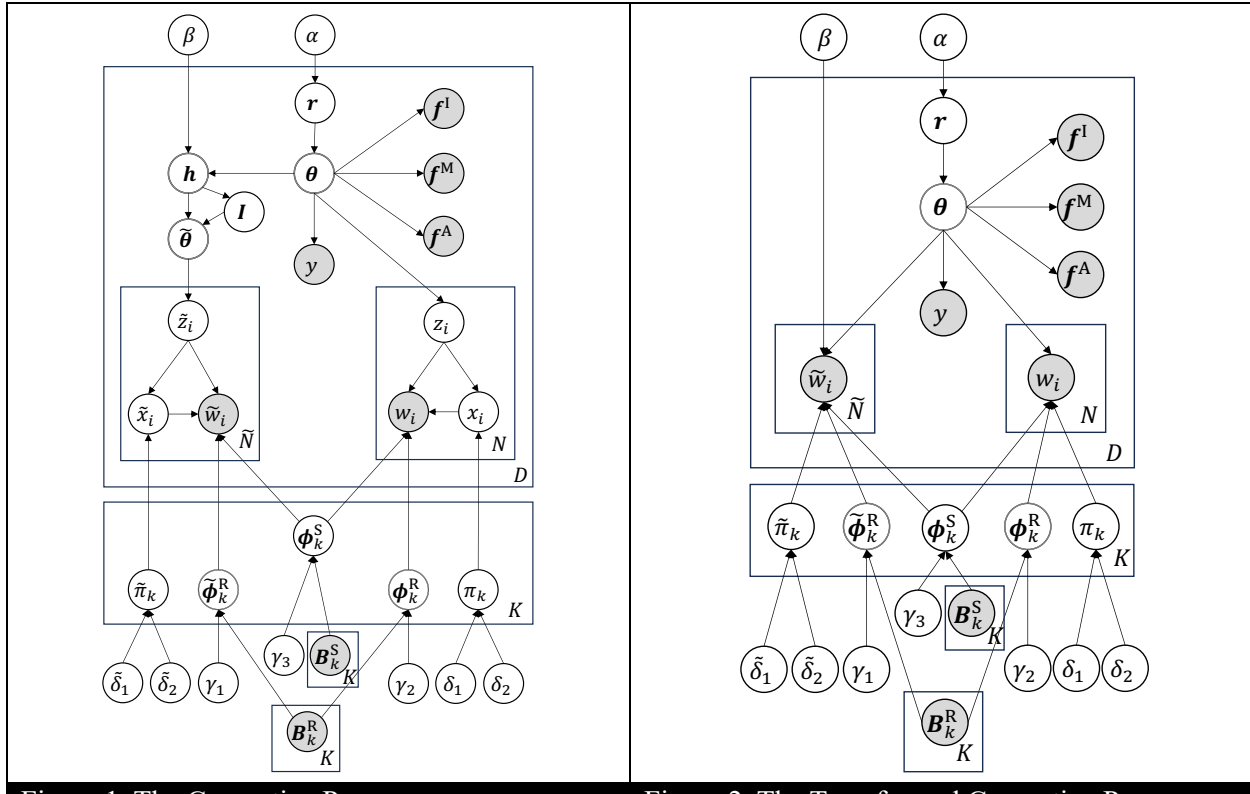


Figure 1. The Generative Process

Figure 2. The Transformed Generative Process

Algorithm 1. The Generative Process

For each topic  $k = 1, \dots, K$ :

Choose  $\pi_k \sim \text{Beta}(\delta_1, \delta_2)$ ,  $\tilde{\pi}_k \sim \text{Beta}(\tilde{\delta}_1, \tilde{\delta}_2)$

For each word  $v$ :

Choose  $\phi_{k,v}^R \sim \text{LogNormal}(B_{k,v}^R, \gamma_1)$ ,  $\tilde{\phi}_{k,v}^R \sim \text{LogNormal}(B_{k,v}^R, \gamma_2)$ ,  $\phi_{k,v}^S \sim \text{LogNormal}(B_{k,v}^S, \gamma_3)$

Normalize  $\phi_{k,v}^R \leftarrow \phi_{k,v}^R / \sum_{v=1}^V \phi_{k,v}^R$ ,  $\tilde{\phi}_{k,v}^R \leftarrow \tilde{\phi}_{k,v}^R / \sum_{v=1}^V \tilde{\phi}_{k,v}^R$ ,  $\phi_{k,v}^S \leftarrow \phi_{k,v}^S / \sum_{v=1}^U \phi_{k,v}^S$

For each video  $d$ :

Choose topic representation  $\mathbf{r}_d \sim \mathcal{N}(\mathbf{r} | \mu_0(\alpha), \text{diag}(\sigma_0^2(\alpha)))$

Generate topic  $\boldsymbol{\theta}_d = \text{softmax}(\mathbf{r}_d)$

Generate drawn probability for each topic:  $\mathbf{h}_d = \beta \cdot \boldsymbol{\theta}_d$

Generate the indicator for remaining topics:  $\mathbf{I}_d \sim \text{Bern}(\mathbf{h}_d)$

Generate topic for transcript:  $\tilde{\boldsymbol{\theta}}_d = \text{Normalize}(\mathbf{h}_d \circ \mathbf{I}_d)$

For each word  $\tilde{w}_i$  in transcript:

Choose a topic:  $\tilde{z}_i \sim \text{Mult}(\tilde{\boldsymbol{\theta}}_d)$

Choose an indicator for choosing seed or regular topic:  $\tilde{x}_i \sim \text{Bern}(\tilde{\pi}_{\tilde{z}_i})$

If  $\tilde{x}_i$  is 1:

Select a word from regular topic  $\tilde{w}_i \sim \text{Mult}(\tilde{\boldsymbol{\phi}}_{\tilde{z}_i}^R)$

If  $\tilde{x}_i$  is 0:

Select a word from seed topic  $\tilde{w}_i \sim \text{Mult}(\boldsymbol{\phi}_{\tilde{z}_i}^S)$

For each word  $w_i$  in comment:

Choose a topic  $z_i \sim \text{Mult}(\boldsymbol{\theta}_d)$

Choose an indicator  $x_i \sim \text{Bern}(\pi_{z_i})$

If  $x_i$  is 1:

Select a word from regular topic  $w_i \sim \text{Mult}(\boldsymbol{\phi}_{z_i}^R)$

If  $x_i$  is 0:

Select a word from seed topic  $w_i \sim \text{Mult}(\boldsymbol{\phi}_{z_i}^S)$

For image, motion, and audio representations:

$\mathbf{f}_d^I = \text{NN}^I(\boldsymbol{\theta}_d)$ ,  $\mathbf{f}_d^M = \text{NN}^M(\boldsymbol{\theta}_d)$ ,  $\mathbf{f}_d^A = \text{NN}^A(\boldsymbol{\theta}_d)$

For label:

$y_d = \text{NN}^L(\boldsymbol{\theta}_d)$

The suboptimal convergence issue is largely attributed to a large number of hidden variables needed to infer. Particularly,  $\tilde{\boldsymbol{\phi}}^R$ ,  $\boldsymbol{\phi}^R$ , and  $\boldsymbol{\phi}^S$  are matrices that contain many, specifically  $(2V + U)K$ , variables. To optimize the convergence, we design a pre-training mechanism, where a classic and easy-to-train model is used to obtain initializations. Particularly, we first leverage a seeded LDA to obtain an initial regular topic-word distribution  $B_{k,v}^R$ ,  $\forall k, v$ , and set it as the prior for  $\tilde{\phi}_{k,v}^R$  and  $\phi_{k,v}^R$ . As each element of  $\tilde{\boldsymbol{\phi}}^R$  and  $\boldsymbol{\phi}^R$  is non-positive, a LogNormal distribution is employed as the prior. Similarly, we obtain an initial seed topic-word distribution  $B_{k,v}^S$  and set it as the prior for  $\phi_{k,v}^S$ . As the word probabilities of a topic sum up to one, normalization is then

adopted. The benefit of this pre-training is that we can train our model from a relatively good starting point, thus effectively addressing the issue of suboptimal convergence.

The above generative process is shown in Algorithm 1, visualized in Figure 1. The shadow nodes represent the observed variables, and the white nodes represent the hidden variables.

### The Transformed Generative Process

The above-mentioned generative process is incompatible with existing deep learning architectures due to the randomness in the process. Particularly, as  $\tilde{z}_i, \tilde{x}_i, z_i, x_i, \tilde{\theta}_d$ , and  $I_d$  are drawn from distributions, we cannot obtain the gradient with respect to model parameters with backpropagation based on those samples, thus complicating the learning process of our model. Hence, it is necessary to reduce the random variables. Therefore, we devise the transformed generative process with the following steps.

1) Reduce  $\tilde{z}_i, \tilde{x}_i, z_i$ , and  $x_i$ : We denote  $\tilde{\phi}^R(\tilde{w}_i)$  as the column that corresponds to word  $\tilde{w}_i$ .  $\tilde{\phi}_k^R(\tilde{w}_i)$  is its element whose column corresponds to word  $\tilde{w}_i$ , and it is in row  $k$  of matrix  $\tilde{\phi}^R$ .  $\tilde{\pi}$  is a vector, each element of which is  $\tilde{\pi}_k$ . For transcripts, given its topic  $\tilde{\theta}_d$ , the probability of generating word  $\tilde{w}_i$  is:

$$\begin{aligned}
p(\tilde{w}_i | \tilde{\theta}_d) &= \sum_{k=1}^K p(\tilde{z}_{d,i} = k | \tilde{\theta}_d) p(\tilde{x}_{d,i} = 1 | \tilde{\pi}_k) \tilde{\phi}_k^R(\tilde{w}_i) + \sum_{k=1}^K p(\tilde{z}_{d,i} = k | \tilde{\theta}_d) p(\tilde{x}_{d,i} = 0 | \tilde{\pi}_k) \phi_k^S(\tilde{w}_i) \\
&= \sum_{k=1}^K \tilde{\theta}_{d,k} \tilde{\pi}_k \tilde{\phi}_k^R(\tilde{w}_i) + \sum_{k=1}^K \tilde{\theta}_{d,k} (1 - \tilde{\pi}_k) \phi_k^S(\tilde{w}_i) \\
&= \left( \tilde{\pi}^T \text{diag}(\tilde{\phi}^R(\tilde{w}_i)) + (\mathbf{1} - \tilde{\pi})^T \text{diag}(\phi^S(\tilde{w}_i)) \right) \tilde{\theta}_d
\end{aligned} \tag{1}$$

In Equation (1),  $p(\tilde{w}_i | \tilde{\theta}_d)$  is computed without involving  $\tilde{z}_i$  or  $\tilde{x}_i$ . Similarly, for  $z_i$  and  $x_i$ , the probability of generating comment word  $w_i$  given video topic  $\theta_d$  can be simplified as:

$$p(w_i | \theta_d) = \left( \pi^T \text{diag}(\phi^R(w_i)) + (\mathbf{1} - \pi)^T \text{diag}(\phi^S(w_i)) \right) \theta_d \tag{2}$$

2) Reduce  $\tilde{\theta}_d$  and  $I_d$ : Equation (1) involves  $\tilde{\theta}_d$ , which are random variables due to the

sampling of  $\mathbf{I}_d$ , given  $\mathbf{h}_d$ . Next, we show how to bypass  $\tilde{\boldsymbol{\theta}}_d$  and  $\mathbf{I}_d$  and directly use  $\mathbf{h}_d$  to compute Equation (1). We denote  $G$  as the space of all possible  $\tilde{\boldsymbol{\theta}}_d$  from  $p(\tilde{\boldsymbol{\theta}}_d | \mathbf{h}_d)$ , then,

$$p(\tilde{w}_i | \mathbf{h}_d) = \sum_{\tilde{\boldsymbol{\theta}}_d \in G} p(\tilde{w}_i | \tilde{\boldsymbol{\theta}}_d) p(\tilde{\boldsymbol{\theta}}_d | \mathbf{h}_d) = \mathbb{E}_{\tilde{\boldsymbol{\theta}}_d \sim p(\tilde{\boldsymbol{\theta}}_d | \mathbf{h}_d)} [p(\tilde{w}_i | \tilde{\boldsymbol{\theta}}_d)] \quad (3)$$

Since it is infeasible to enumerate  $\tilde{\boldsymbol{\theta}}_d$ , we resort to the Monto Carlo method to approximate  $p(\tilde{w}_i | \mathbf{h}_d)$ . Specifically, we sample a number of ( $N_M$ ) for  $\tilde{\boldsymbol{\theta}}_d$  from  $p(\tilde{\boldsymbol{\theta}}_d | \mathbf{h}_d)$  and each sample is denoted as  $\tilde{\boldsymbol{\theta}}_d^{(n)}$ . Equation (3) can be transformed to:

$$p(\tilde{w}_i | \mathbf{h}_d) \approx \frac{1}{N_M} \sum_{n=1}^{N_M} p(\tilde{w}_i | \tilde{\boldsymbol{\theta}}_d^{(n)}) = \left( \tilde{\boldsymbol{\pi}}^T \text{diag}(\tilde{\boldsymbol{\phi}}^R(\tilde{w}_i)) + (\mathbf{1} - \tilde{\boldsymbol{\pi}})^T \text{diag}(\boldsymbol{\phi}^S(\tilde{w}_i)) \right) \left( \frac{1}{N_M} \sum_{n=1}^{N_M} \tilde{\boldsymbol{\theta}}_d^{(n)} \right) \quad (4)$$

Note that when  $N_M \rightarrow \infty$ , according to the Monto Carlo method's property, the approximation converges to the expectation, i.e.,

$$p(\tilde{w}_i | \mathbf{h}_d) = \left( \tilde{\boldsymbol{\pi}}^T \text{diag}(\tilde{\boldsymbol{\phi}}^R(\tilde{w}_i)) + (\mathbf{1} - \tilde{\boldsymbol{\pi}})^T \text{diag}(\boldsymbol{\phi}^S(\tilde{w}_i)) \right) \left( \frac{1}{N_M} \sum_{n=1}^{N_M \rightarrow \infty} \tilde{\boldsymbol{\theta}}_d^{(n)} \right) \quad (5)$$

where  $\frac{1}{N_M} \sum_{n=1}^{N_M \rightarrow \infty} \tilde{\boldsymbol{\theta}}_d^{(n)}$  can be seen as the expectation of  $\tilde{\boldsymbol{\theta}}_d$ , i.e.,  $\mathbb{E}_{\tilde{\boldsymbol{\theta}}_d \sim p(\tilde{\boldsymbol{\theta}}_d | \mathbf{h}_d)} \tilde{\boldsymbol{\theta}}_d$ . Accordingly,

$$p(\tilde{w}_i | \mathbf{h}_d) = \left( \tilde{\boldsymbol{\pi}}^T \text{diag}(\tilde{\boldsymbol{\phi}}^R(\tilde{w}_i)) + (\mathbf{1} - \tilde{\boldsymbol{\pi}})^T \text{diag}(\boldsymbol{\phi}^S(\tilde{w}_i)) \right) \mathbb{E}_{\tilde{\boldsymbol{\theta}}_d \sim p(\tilde{\boldsymbol{\theta}}_d | \mathbf{h}_d)} \tilde{\boldsymbol{\theta}}_d \quad (6)$$

**Theorem:** Assuming there are variables  $I_d^k, k = 1, \dots, K$ , and each  $I_d^k$  follows  $\text{Bernoulli}(h_d^k)$ .

We compute a normalized variable  $\tilde{\boldsymbol{\theta}}_d$  whose  $k$ -th element  $\tilde{\theta}_d^k$  is  $\frac{h_d^k}{\sum_{i=1}^K h_d^i \cdot I_d^i}$  if  $I_d^k = 1$  and is 0 if  $I_d^k = 0$ . Then,  $(h_d^k)^2 \frac{1}{h_d^k + \sum_{i=1, i \neq k}^K (h_d^i)^2}$  is a lower bound of the expectation of  $\tilde{\theta}_d^k$ . Collectively,

$$\mathbb{E}_{\tilde{\boldsymbol{\theta}}_d \sim p(\tilde{\boldsymbol{\theta}}_d | \mathbf{h}_d)} \tilde{\boldsymbol{\theta}}_d \geq \left[ \frac{(h_d^1)^2}{h_d^1 + \sum_{i=1, i \neq 1}^K (h_d^i)^2}, \dots, \frac{(h_d^k)^2}{h_d^k + \sum_{i=1, i \neq k}^K (h_d^i)^2}, \dots, \frac{(h_d^K)^2}{h_d^K + \sum_{i=1, i \neq K}^K (h_d^i)^2} \right]^T \quad (7)$$

The proof of this theorem is included in Appendix 2.

We denote the lower bound of Equation (7) as  $\mathbf{b}_d$ . As each element of  $\tilde{\boldsymbol{\pi}}, \tilde{\boldsymbol{\phi}}^R(\tilde{w}_i)$ , and

$\boldsymbol{\phi}^S(\tilde{w}_i)$  is non-negative and no larger than 1, each element of  $\tilde{\boldsymbol{\pi}}^T \text{diag}(\tilde{\boldsymbol{\phi}}^R(\tilde{w}_i)) + (\mathbf{1} - \tilde{\boldsymbol{\pi}})^T \text{diag}(\boldsymbol{\phi}^S(\tilde{w}_i))$  is non-negative. Meanwhile, as each element of  $\mathbf{b}_d$  and  $\tilde{\boldsymbol{\theta}}_d$  is non-negative, Equation (6) can be transformed to:

$$p(\tilde{w}_i | \mathbf{h}_d) \geq \left( \tilde{\boldsymbol{\pi}}^T \text{diag}(\tilde{\boldsymbol{\phi}}^R(\tilde{w}_i)) + (\mathbf{1} - \tilde{\boldsymbol{\pi}})^T \text{diag}(\boldsymbol{\phi}^S(\tilde{w}_i)) \right) \mathbf{b}_d \quad (8)$$

Now the computation of  $p(\tilde{w}_i | \mathbf{h}_d)$  does not involve  $\tilde{\boldsymbol{\theta}}_d$ , but involves  $\mathbf{b}_d$ , which is composed of  $\mathbf{h}_d$ . This overcomes the randomness problem due to the drawing of  $\tilde{\boldsymbol{\theta}}_d$  and  $\mathbf{I}_d$ . Take one step further, as  $\mathbf{h}_d = \beta \cdot \boldsymbol{\theta}_d$ ,  $p(\tilde{w}_i | \mathbf{h}_d)$  can be expressed as  $p(\tilde{w}_i | \boldsymbol{\theta}_d)$  by replacing  $\mathbf{h}_d$  with  $\beta \cdot \boldsymbol{\theta}_d$ :

$$p(\tilde{w}_i | \boldsymbol{\theta}_d) \geq \left( \tilde{\boldsymbol{\pi}}^T \text{diag}(\tilde{\boldsymbol{\phi}}^R(\tilde{w}_i)) + (\mathbf{1} - \tilde{\boldsymbol{\pi}})^T \text{diag}(\boldsymbol{\phi}^S(\tilde{w}_i)) \right) \mathbf{b}'_d \quad (9)$$

where the  $k$ -th element of  $\mathbf{b}'_d$  is expressed as:

$$\mathbf{b}'_d^k = (\beta \theta_d^k)^2 \frac{1}{\beta \theta_d^k + \sum_{i=1, i \neq k}^K (\beta \theta_d^i)^2} = (\theta_d^k)^2 \frac{1}{\theta_d^k / \beta + \sum_{i=1, i \neq k}^K (\theta_d^i)^2} \quad (10)$$

By reducing  $\tilde{z}_i, \tilde{x}_i, z_i, x_i, \tilde{\boldsymbol{\theta}}_d$ , and  $\mathbf{I}_d$  with the above two steps, we generate words  $\tilde{w}_i$  and  $w_i$  with a simplified process, named the transformed generative process (Figure 2). The advantage of this transformed generative process is that it not only keeps the advantages of the original generative process (e.g., multi-origin topics, automated seed supervision, etc.), but also is compatible with deep learning because the errors can be backpropagated to learn our model.

### The Variational Inference Method for the Proposed Model

In the transformed generative process, the observed variables include  $\tilde{\mathbf{w}}_d, \mathbf{w}_d, \mathbf{f}_d^I, \mathbf{f}_d^M, \mathbf{f}_d^A$ , and  $y_d, \forall d$ . The hidden variables include  $\tilde{\boldsymbol{\pi}}, \boldsymbol{\pi}, \boldsymbol{\phi}^S, \boldsymbol{\phi}^R, \tilde{\boldsymbol{\phi}}^R, \mathbf{r}_d$ , and  $\boldsymbol{\theta}_d, \forall d$ . The topics  $\boldsymbol{\theta}_d$  play a pivotal role in determining a video's depressive impact and in explaining what risk factors a video contains. Hence, we need to infer  $\boldsymbol{\theta}_d$  given the observed variables. We also need to infer  $\tilde{\boldsymbol{\pi}}, \boldsymbol{\pi}, \boldsymbol{\phi}^S, \boldsymbol{\phi}^R, \tilde{\boldsymbol{\phi}}^R$  because  $\tilde{\boldsymbol{\pi}}$  and  $\boldsymbol{\pi}$  inform us the degree of each topic coming from existing medical

knowledge or social media context, while  $\boldsymbol{\phi}^S$ ,  $\boldsymbol{\phi}^R$ , and  $\tilde{\boldsymbol{\phi}}^R$  help to interpret the meaning of topics. Formally, we aim to obtain the posterior distribution  $p(\boldsymbol{\Theta}, \tilde{\boldsymbol{\pi}}, \boldsymbol{\pi}, \boldsymbol{\phi}^S, \boldsymbol{\phi}^R, \tilde{\boldsymbol{\phi}}^R | \tilde{\mathbf{W}}, \mathbf{W}, \mathbf{F}^I, \mathbf{F}^M, \mathbf{F}^A, \mathbf{Y})$ , where  $\boldsymbol{\Theta}$  is the collection of  $\boldsymbol{\Theta}_d$  from each video  $d$ . However, the posterior distribution is intractable. Hence, we adopt the variational inference which introduces a variational distribution  $q_{\boldsymbol{\Psi}}(\boldsymbol{\Theta}, \tilde{\boldsymbol{\pi}}, \boldsymbol{\pi}, \boldsymbol{\phi}^S, \boldsymbol{\phi}^R, \tilde{\boldsymbol{\phi}}^R | \tilde{\mathbf{W}}, \mathbf{W}, \mathbf{F}^I, \mathbf{F}^M, \mathbf{F}^A, \mathbf{Y})$  to approximate the posterior distribution. We simplify the notion of the variational distribution as  $q_{\boldsymbol{\Psi}}(\boldsymbol{\Theta}, \tilde{\boldsymbol{\pi}}, \boldsymbol{\pi}, \boldsymbol{\phi}^S, \boldsymbol{\phi}^R, \tilde{\boldsymbol{\phi}}^R)$ . The form and the parameter  $\boldsymbol{\Psi}$  of the variational distribution greatly impact the approximation results. The same as NTMs, we employ neural networks as variation distributions to infer the values of the hidden variables. In this study, the neural network is referred to as the inference network. In this case, the parameters  $\boldsymbol{\Psi}$  refers to the parameters of the neural network, and we can update  $\boldsymbol{\Psi}$  the same as deep learning models.

### Evidence Lower Bound (ELBO)

We minimize the KL divergence between the variational and the posterior distributions to push the variational distribution towards the posterior. Denoting it as  $\text{KL}^{\text{ALL}}$ , we prove (Appendix 3):

$$\begin{aligned} \text{KL}^{\text{ALL}} &= \mathbb{E}_{q_{\boldsymbol{\Psi}}} [\log q_{\boldsymbol{\Psi}}(\boldsymbol{\Theta}, \tilde{\boldsymbol{\pi}}, \boldsymbol{\pi}, \boldsymbol{\phi}^S, \boldsymbol{\phi}^R, \tilde{\boldsymbol{\phi}}^R) - \log p(\boldsymbol{\Theta}, \tilde{\boldsymbol{\pi}}, \boldsymbol{\pi}, \boldsymbol{\phi}^S, \boldsymbol{\phi}^R, \tilde{\boldsymbol{\phi}}^R, \tilde{\mathbf{W}}, \mathbf{W}, \mathbf{F}^I, \mathbf{F}^M, \mathbf{F}^A, \mathbf{Y})] \\ &\quad + \log p(\tilde{\mathbf{W}}, \mathbf{W}, \mathbf{F}^I, \mathbf{F}^M, \mathbf{F}^A, \mathbf{Y}) \end{aligned} \quad (11)$$

As the value of the KL divergence is non-negative, the ELBO, which is the lower bound of the log-likelihood of observations  $\log p(\tilde{\mathbf{W}}, \mathbf{W}, \mathbf{F}^I, \mathbf{F}^M, \mathbf{F}^A, \mathbf{Y})$  (called evidence), is defined as:

$$\begin{aligned} \text{ELBO} &\triangleq \log p(\tilde{\mathbf{W}}, \mathbf{W}, \mathbf{F}^I, \mathbf{F}^M, \mathbf{F}^A, \mathbf{Y}) - \text{KL}^{\text{ALL}} \\ &= \mathbb{E}_{q_{\boldsymbol{\Psi}}} [\log p(\boldsymbol{\Theta}, \tilde{\boldsymbol{\pi}}, \boldsymbol{\pi}, \boldsymbol{\phi}^S, \boldsymbol{\phi}^R, \tilde{\boldsymbol{\phi}}^R, \tilde{\mathbf{W}}, \mathbf{W}, \mathbf{F}^I, \mathbf{F}^M, \mathbf{F}^A, \mathbf{Y}) \\ &\quad - \log q_{\boldsymbol{\Psi}}(\boldsymbol{\Theta}, \tilde{\boldsymbol{\pi}}, \boldsymbol{\pi}, \boldsymbol{\phi}^S, \boldsymbol{\phi}^R, \tilde{\boldsymbol{\phi}}^R)] \end{aligned} \quad (12)$$

As the evidence is fixed, minimizing the KL divergence is equivalent to maximizing ELBO. ELBO can be further derived as (proof in Appendix 4):

$$\begin{aligned} \text{ELBO} = & \mathbb{E}_{q_{\Psi}}[\log p(\widetilde{\mathbf{W}}, \mathbf{W}, \mathbf{F}^I, \mathbf{F}^M, \mathbf{F}^A, \mathbf{Y} | \boldsymbol{\theta}, \widetilde{\boldsymbol{\pi}}, \boldsymbol{\pi}, \boldsymbol{\phi}^S, \boldsymbol{\phi}^R, \widetilde{\boldsymbol{\phi}}^R)] \\ & - \text{KL}(q_{\Psi}(\boldsymbol{\theta}, \widetilde{\boldsymbol{\pi}}, \boldsymbol{\pi}, \boldsymbol{\phi}^S, \boldsymbol{\phi}^R, \widetilde{\boldsymbol{\phi}}^R) \| p(\boldsymbol{\theta}, \widetilde{\boldsymbol{\pi}}, \boldsymbol{\pi}, \boldsymbol{\phi}^S, \boldsymbol{\phi}^R, \widetilde{\boldsymbol{\phi}}^R)) \end{aligned} \quad (13)$$

where  $p(\boldsymbol{\theta}, \widetilde{\boldsymbol{\pi}}, \boldsymbol{\pi}, \boldsymbol{\phi}^S, \boldsymbol{\phi}^R, \widetilde{\boldsymbol{\phi}}^R)$  denotes the prior distribution.

### The First Term of ELBO

As videos are independent,  $p(\widetilde{\mathbf{W}}, \mathbf{W}, \mathbf{F}^I, \mathbf{F}^M, \mathbf{F}^A, \mathbf{Y} | \boldsymbol{\theta}, \widetilde{\boldsymbol{\pi}}, \boldsymbol{\pi}, \boldsymbol{\phi}^S, \boldsymbol{\phi}^R, \widetilde{\boldsymbol{\phi}}^R)$  in first term equals to:

$$\begin{aligned} & p(\widetilde{\mathbf{W}}, \mathbf{W}, \mathbf{F}^I, \mathbf{F}^M, \mathbf{F}^A, \mathbf{Y} | \boldsymbol{\theta}, \widetilde{\boldsymbol{\pi}}, \boldsymbol{\pi}, \boldsymbol{\phi}^S, \boldsymbol{\phi}^R, \widetilde{\boldsymbol{\phi}}^R) \\ & = \prod_{d=1}^D p(\widetilde{\mathbf{w}}_d, \mathbf{w}_d, \mathbf{f}_d^I, \mathbf{f}_d^M, \mathbf{f}_d^A, y_d | \boldsymbol{\theta}_d, \widetilde{\boldsymbol{\pi}}, \boldsymbol{\pi}, \boldsymbol{\phi}^S, \boldsymbol{\phi}^R, \widetilde{\boldsymbol{\phi}}^R) \end{aligned} \quad (14)$$

Leveraging the conditional independence relationships in the transformed generative process, each  $p(\widetilde{\mathbf{w}}_d, \mathbf{w}_d, \mathbf{f}_d^I, \mathbf{f}_d^M, \mathbf{f}_d^A, y_d | \boldsymbol{\theta}_d, \widetilde{\boldsymbol{\pi}}, \boldsymbol{\pi}, \boldsymbol{\phi}^S, \boldsymbol{\phi}^R, \widetilde{\boldsymbol{\phi}}^R)$  in Equation (14) can be further factorized as:

$$\prod_{i=1}^{\tilde{N}_d} p(\tilde{w}_{d,i} | \boldsymbol{\theta}_d, \widetilde{\boldsymbol{\pi}}, \widetilde{\boldsymbol{\phi}}^R, \boldsymbol{\phi}^S) \prod_{i=1}^{N_d} p(w_{d,i} | \boldsymbol{\theta}_d, \boldsymbol{\pi}, \boldsymbol{\phi}^R, \boldsymbol{\phi}^S) p(y_d | \boldsymbol{\theta}_d) p(\mathbf{f}_d^I | \boldsymbol{\theta}_d) p(\mathbf{f}_d^M | \boldsymbol{\theta}_d) p(\mathbf{f}_d^A | \boldsymbol{\theta}_d) \quad (15)$$

where  $\tilde{N}_d$  ( $N_d$ ) is the number of words in the video  $d$ 's transcript (comment). The logarithm is:

$$\begin{aligned} & \sum_{i=1}^{\tilde{N}_d} \log p(\tilde{w}_{d,i} | \boldsymbol{\theta}_d, \widetilde{\boldsymbol{\pi}}, \widetilde{\boldsymbol{\phi}}^R, \boldsymbol{\phi}^S) + \sum_{i=1}^{N_d} \log p(w_{d,i} | \boldsymbol{\theta}_d, \boldsymbol{\pi}, \boldsymbol{\phi}^R, \boldsymbol{\phi}^S) + \log p(y_d | \boldsymbol{\theta}_d) + \log p(\mathbf{f}_d^I | \boldsymbol{\theta}_d) \\ & + \log p(\mathbf{f}_d^M | \boldsymbol{\theta}_d) + \log p(\mathbf{f}_d^A | \boldsymbol{\theta}_d) \end{aligned} \quad (16)$$

For the first term in Equation (16), as  $p(\tilde{w}_{d,i} | \boldsymbol{\theta}_d, \widetilde{\boldsymbol{\pi}}, \widetilde{\boldsymbol{\phi}}^R, \boldsymbol{\phi}^S) \geq \left( \widetilde{\boldsymbol{\pi}}^T \text{diag}(\widetilde{\boldsymbol{\phi}}^R(\tilde{w}_i)) + (\mathbf{1} - \widetilde{\boldsymbol{\pi}})^T \text{diag}(\boldsymbol{\phi}^S(\tilde{w}_i)) \right) \mathbf{b}'_d$ , we can replace  $p(\tilde{w}_{d,i} | \boldsymbol{\theta}_d, \widetilde{\boldsymbol{\pi}}, \widetilde{\boldsymbol{\phi}}^R, \boldsymbol{\phi}^S)$  with this lower bound.

According to Equation (2), the second term in Equation (16) can be transformed to:

$$\sum_{i=1}^{N_d} \log p(w_{d,i} | \boldsymbol{\theta}_d, \boldsymbol{\pi}, \boldsymbol{\phi}^R, \boldsymbol{\phi}^S) = \sum_{i=1}^{N_d} \log \left[ \left( \boldsymbol{\pi}^T \text{diag}(\boldsymbol{\phi}^R(w_i)) + (\mathbf{1} - \boldsymbol{\pi})^T \text{diag}(\boldsymbol{\phi}^S(w_i)) \right) \boldsymbol{\theta}_d \right] \quad (17)$$

For the third term in Equation (16),  $\log p(y_d | \boldsymbol{\theta}_d)$ , we adopt a neural network with sigmoid for the prediction,  $NN^L$ , where  $p(y_d = 1 | \boldsymbol{\theta}_d) = NN^L(\boldsymbol{\theta}_d)$ . As  $y_d$  is 0 or 1, thus  $\log p(y_d | \boldsymbol{\theta}_d) =$

$y_d NN^L(\boldsymbol{\theta}_d) + (1 - y) \left( 1 - NN^L(\boldsymbol{\theta}_d) \right) = -\text{CE} \left( y_d, NN^L(\boldsymbol{\theta}_d) \right)$ , where CE refers to cross entropy, a common classification measure. Therefore, we also include the depressive impact prediction in this process.

For the fourth term in Equation (16),  $\log p(\mathbf{f}_d^I | \boldsymbol{\theta}_d)$ , we adopt the same approach as VAEs, where the probability is represented as the distance between the reconstructed vector (denoted as  $NN^I(\boldsymbol{\theta}_d)$ ) and the ground truth vector  $\mathbf{f}_d^I$ . Hence, maximizing  $\log p(\mathbf{f}_d^I | \boldsymbol{\theta}_d)$  is reduced to minimizing the reconstruction loss. Therefore, we replace  $\log p(\mathbf{f}_d^I | \boldsymbol{\theta}_d)$  by  $-\xi^I \|\mathbf{f}_d^I - NN^I(\boldsymbol{\theta}_d)\|_2$ , where  $\xi^I$  is the weight to control the importance of reconstructing image features compared with other parts. Similar operations apply to maximizing the last two terms in Equation (16),  $\log p(\mathbf{f}_d^M | \boldsymbol{\theta}_d)$  and  $\log p(\mathbf{f}_d^A | \boldsymbol{\theta}_d)$ . Taken together, the probability part in the first term of Equation (13) can be transformed to:

$$\begin{aligned} & \log p(\widetilde{\mathbf{W}}, \mathbf{W}, \mathbf{F}^I, \mathbf{F}^M, \mathbf{F}^A, \mathbf{Y} | \boldsymbol{\theta}, \widetilde{\boldsymbol{\pi}}, \boldsymbol{\pi}, \boldsymbol{\phi}^S, \boldsymbol{\phi}^R, \widetilde{\boldsymbol{\phi}}^R) \\ & \geq \sum_{d=1}^D \left( \sum_{i=1}^{\tilde{N}_d} \log \left[ \left( \boldsymbol{\pi}^T \text{diag} \left( \boldsymbol{\phi}^R(w_i) \right) + (\mathbf{1} - \boldsymbol{\pi})^T \text{diag} \left( \boldsymbol{\phi}^S(w_i) \right) \right) \mathbf{b}'_d \right] \right. \\ & \quad \left. + \sum_{i=1}^{N_d} \log \left[ \left( \boldsymbol{\pi}^T \text{diag} \left( \boldsymbol{\phi}^R(w_i) \right) + (\mathbf{1} - \boldsymbol{\pi})^T \text{diag} \left( \boldsymbol{\phi}^S(w_i) \right) \right) \boldsymbol{\theta}_d \right] - \text{CE} \left( y_d, NN^L(\boldsymbol{\theta}_d) \right) \right. \\ & \quad \left. - \xi^I \|\mathbf{f}_d^I - NN^I(\boldsymbol{\theta}_d)\|_2 - \xi^M \|\mathbf{f}_d^M - NN^M(\boldsymbol{\theta}_d)\|_2 - \xi^A \|\mathbf{f}_d^A - NN^A(\boldsymbol{\theta}_d)\|_2 \right) \end{aligned} \quad (18)$$

Equation (18) generates a lower bound for ELBO in Equation (13). By maximizing this lower bound, and the value of ELBO is expected to increase at the same time. Now consider the first term of Equation (13) with the expectation, we adopt the Monte Carlo method to obtain samples of  $\boldsymbol{\theta}$ ,  $\widetilde{\boldsymbol{\pi}}$ ,  $\widetilde{\boldsymbol{\phi}}^R$ ,  $\boldsymbol{\phi}^S$ ,  $\boldsymbol{\pi}$ , and  $\boldsymbol{\phi}^R$  from variational distributions and then estimate the expectation based on the drawn samples. We will articulate the variational distributions later.

## The Second Term of ELBO

As suggested by the mean-field approximation methods, each variable (i.e.,  $\boldsymbol{\Theta}$ ,  $\tilde{\boldsymbol{\pi}}$ ,  $\tilde{\boldsymbol{\phi}}^R$ ,  $\boldsymbol{\phi}^S$ ,  $\boldsymbol{\pi}$ , and  $\boldsymbol{\phi}^R$ ) in the variation distribution  $q_{\boldsymbol{\psi}}$  is assumed to be independent. As a common practice, the prior distribution of each variable is set independently without considering others, which makes the priors independent. Hence, the second term in Equation (13) can be decomposed as:

$$\begin{aligned} \text{KL}(q_{\boldsymbol{\psi}}(\boldsymbol{\Theta}, \tilde{\boldsymbol{\pi}}, \boldsymbol{\pi}, \boldsymbol{\phi}^S, \boldsymbol{\phi}^R, \tilde{\boldsymbol{\phi}}^R) \| p(\boldsymbol{\Theta}, \tilde{\boldsymbol{\pi}}, \boldsymbol{\pi}, \boldsymbol{\phi}^S, \boldsymbol{\phi}^R, \tilde{\boldsymbol{\phi}}^R)) \\ = \text{KL}(q_{\boldsymbol{\psi}}(\boldsymbol{\Theta}) \| p(\boldsymbol{\Theta})) + \text{KL}(q_{\boldsymbol{\psi}}(\tilde{\boldsymbol{\pi}}) \| p(\tilde{\boldsymbol{\pi}})) + \text{KL}(q_{\boldsymbol{\psi}}(\tilde{\boldsymbol{\phi}}^R) \| p(\tilde{\boldsymbol{\phi}}^R)) \\ + \text{KL}(q_{\boldsymbol{\psi}}(\boldsymbol{\phi}^S) \| p(\boldsymbol{\phi}^S)) + \text{KL}(q_{\boldsymbol{\psi}}(\boldsymbol{\pi}) \| p(\boldsymbol{\pi})) + \text{KL}(q_{\boldsymbol{\psi}}(\boldsymbol{\phi}^R) \| p(\boldsymbol{\phi}^R)) \end{aligned} \quad (19)$$

where  $p(\boldsymbol{\Theta})$  is the prior distribution for  $\boldsymbol{\Theta}$ . Similar notations apply to the others.

For the first term  $\text{KL}(q_{\boldsymbol{\psi}}(\boldsymbol{\Theta}) \| p(\boldsymbol{\Theta}))$ , as each video is independent and  $\boldsymbol{\theta}_d$  is the softmax of  $\mathbf{r}_d$ ,

$$\text{KL}(q_{\boldsymbol{\psi}}(\boldsymbol{\Theta}) \| p(\boldsymbol{\Theta})) = \sum_{d=1}^D \text{KL}(q_{\boldsymbol{\psi}}(\boldsymbol{\theta}_d) \| p(\boldsymbol{\theta}_d)) = \sum_{d=1}^D \text{KL}(q_{\boldsymbol{\psi}}(\mathbf{r}_d) \| p(\mathbf{r}_d)) \quad (20)$$

where  $p(\mathbf{r}_d)$  is the prior distribution of  $\mathbf{r}_d$ , which is defined as  $\mathcal{N}(\mathbf{r} | \mu_0(\alpha), \text{diag}(\sigma_0^2(\alpha)))$ . As suggested by prior studies (Hennig et al. 2012), we set  $\mu_0(\alpha) = 0$  and  $\sigma_0^2(\alpha) = (K-1)/(\alpha K)$ . As the inference for  $\mathbf{r}_d$  requires the video's all observed variables  $\tilde{\mathbf{w}}_d$ ,  $\mathbf{w}_d$ ,  $\mathbf{f}_d^I$ ,  $\mathbf{f}_d^M$ ,  $\mathbf{f}_d^A$ , and  $y_d$ , the inference network for the variational distribution of  $\mathbf{r}_d$  is designed as:

$$\boldsymbol{\mu}_d = \text{NN}^{\text{mean}}(\tilde{\mathbf{w}}_d, \mathbf{w}_d, \mathbf{f}_d^I, \mathbf{f}_d^M, \mathbf{f}_d^A, y_d) \quad (21)$$

$$\boldsymbol{\sigma}_d = \text{NN}^{\text{std}}(\tilde{\mathbf{w}}_d, \mathbf{w}_d, \mathbf{f}_d^I, \mathbf{f}_d^M, \mathbf{f}_d^A, y_d) \quad (22)$$

$$\mathbf{r}_d \sim \mathcal{N}(\boldsymbol{\mu}_d, \text{diag}(\boldsymbol{\sigma}_d^2)) \quad (23)$$

Then, the  $\text{KL}(q_{\boldsymbol{\psi}}(\mathbf{r}_d) \| p(\mathbf{r}_d))$  in Equation (20) is computed as:

$$\begin{aligned} \text{KL}(q_{\boldsymbol{\psi}}(\mathbf{r}_d) \| p(\mathbf{r}_d)) &= \text{KL}\left(\mathcal{N}(\boldsymbol{\mu}_d, \text{diag}(\boldsymbol{\sigma}_d^2)) \middle\| \mathcal{N}\left(\mu_0(\alpha), \text{diag}(\sigma_0^2(\alpha))\right)\right) \\ &= \frac{1}{2} \left[ \log \frac{|\text{diag}(\sigma_0^2(\alpha))|}{|\text{diag}(\boldsymbol{\sigma}_d^2)|} - K + (\mu_0(\alpha) - \boldsymbol{\mu}_d)^T \text{diag}(\sigma_0^2(\alpha))^{-1} (\mu_0(\alpha) - \boldsymbol{\mu}_d) \right. \\ &\quad \left. + \text{tr}\left(\text{diag}(\sigma_0^2(\alpha))^{-1} \text{diag}(\boldsymbol{\sigma}_d^2)\right) \right] \end{aligned} \quad (24)$$

For the second term  $\text{KL}(q_{\boldsymbol{\psi}}(\tilde{\boldsymbol{\pi}}) \| p(\tilde{\boldsymbol{\pi}}))$ , as  $\tilde{\boldsymbol{\pi}}$  is conditionally independent of  $\mathbf{W}$ ,  $\mathbf{F}^I$ ,  $\mathbf{F}^M$ ,  $\mathbf{F}^A$ , and  $\mathbf{Y}$  given  $\tilde{\mathbf{W}}$ , we incorporate this conditional independence relationship in the variational

distribution, i.e.,  $q_{\psi}(\tilde{\boldsymbol{\pi}}|\tilde{\mathbf{W}}, \mathbf{W}, \mathbf{F}^I, \mathbf{F}^M, \mathbf{F}^A, \mathbf{Y}) = q_{\psi}(\tilde{\boldsymbol{\pi}}|\tilde{\mathbf{W}})$ . Hence, we feed  $\tilde{\mathbf{W}}$  into an inference network to approximate the posterior distribution. Formally,  $\tilde{\sigma}_1^{\text{pos}} = NN^{\tilde{\delta}_1}(\tilde{\mathbf{W}})$ ,  $\tilde{\sigma}_2^{\text{pos}} = NN^{\tilde{\delta}_2}(\tilde{\mathbf{W}})$ , and then the variation distribution is  $\text{Beta}(\tilde{\delta}_1^{\text{pos}}, \tilde{\delta}_2^{\text{pos}})$ . The prior is  $\text{Beta}(\tilde{\delta}_1, \tilde{\delta}_2)$ . As suggested by prior studies (Jagarlamudi et al. 2012), we set  $\tilde{\delta}_1$  as 1 and  $\tilde{\delta}_2$  as 1. The KL divergence is:

$$\begin{aligned}
\text{KL}(q_{\psi}(\tilde{\boldsymbol{\pi}})\|p(\tilde{\boldsymbol{\pi}})) &= \text{KL}(\text{Beta}(\tilde{\delta}_1^{\text{pos}}, \tilde{\delta}_2^{\text{pos}})\|\text{Beta}(\tilde{\delta}_1, \tilde{\delta}_2)) \\
&= \log \frac{B(\tilde{\delta}_1, \tilde{\delta}_2)}{B(\tilde{\delta}_1^{\text{pos}}, \tilde{\delta}_2^{\text{pos}})} \\
&\quad + (\tilde{\delta}_1^{\text{pos}} - \tilde{\delta}_1) \left( \psi(\tilde{\delta}_1^{\text{pos}}) - \psi(\tilde{\delta}_1^{\text{pos}} + \tilde{\delta}_2^{\text{pos}}) \right) \\
&\quad + (\tilde{\delta}_2^{\text{pos}} - \tilde{\delta}_2) \left( \psi(\tilde{\delta}_2^{\text{pos}}) - \psi(\tilde{\delta}_1^{\text{pos}} + \tilde{\delta}_2^{\text{pos}}) \right)
\end{aligned} \tag{25}$$

where  $B$  is the Beta function and  $\psi$  is the digamma function.

Similarly, for  $\text{KL}(q_{\psi}(\boldsymbol{\pi})\|p(\boldsymbol{\pi}))$ , the variational distribution  $q_{\psi}(\boldsymbol{\pi}|\tilde{\mathbf{W}}, \mathbf{W}, \mathbf{F}^I, \mathbf{F}^M, \mathbf{F}^A, \mathbf{Y})$  can be simplified as  $q_{\psi}(\boldsymbol{\pi}|\mathbf{W})$ . We feed  $\mathbf{W}$  into the inference networks to obtain the variational distribution  $\text{Beta}(\delta_1^{\text{pos}}, \delta_2^{\text{pos}})$ , where  $\delta_1^{\text{pos}} = NN^{\delta_1}(\mathbf{W})$ ,  $\delta_2^{\text{pos}} = NN^{\delta_2}(\mathbf{W})$ . Similarly, we set  $\delta_1^{\text{pos}}$  and  $\delta_2^{\text{pos}}$  as 1. The KL divergence is computed similar to Equation (25).

For the third term  $\text{KL}(q_{\psi}(\tilde{\boldsymbol{\phi}}^R)\|p(\tilde{\boldsymbol{\phi}}^R))$ , as the  $\tilde{\boldsymbol{\phi}}^R$  is conditionally independent of  $\mathbf{W}, \mathbf{F}^I, \mathbf{F}^M, \mathbf{F}^A$ , and  $\mathbf{Y}$  given  $\tilde{\mathbf{W}}$ , the inference network takes  $\tilde{\mathbf{W}}$  as the input. As each element in  $\tilde{\boldsymbol{\phi}}^R$  is non-negative, we assume that the variational distribution for each element follows the LogNormal distribution and its parameters are obtained with neural networks, i.e.,

$\text{LogNormal}\left(NN^{\tilde{\mu}}(\tilde{\mathbf{W}})_{k,v}, NN^{\tilde{\sigma}}(\tilde{\mathbf{W}})_{k,v}\right)$ , where  $NN^{\tilde{\mu}}(\tilde{\mathbf{W}})_{k,v}$  denotes the element at the  $k$ -th row and  $v$ -th column in matrix  $NN^{\tilde{\mu}}(\tilde{\mathbf{W}})$ . Similar notations apply to  $NN^{\tilde{\sigma}}(\tilde{\mathbf{W}})_{k,v}$ . The prior is  $\text{LogNormal}(B_{k,v}^R, \gamma_1)$ . As suggested by prior studies (Hennig et al. 2012), we set  $B_{k,v}^R$  as 0 and  $\gamma_1$  as  $(VK - 1)/(VK)$ . Hence, we have:

$$\begin{aligned}
\text{KL}(q_{\psi}(\tilde{\boldsymbol{\phi}}^R) \| p(\tilde{\boldsymbol{\phi}}^R)) &= \sum_{k=1}^K \sum_{v=1}^V \text{KL} \left( \text{LogNormal} \left( NN^{\tilde{\mu}}(\tilde{\mathbf{W}})_{k,v}, NN^{\tilde{\sigma}}(\tilde{\mathbf{W}})_{k,v} \right) \| \text{LogNormal}(B_{k,v}^R, \gamma_1) \right) \\
&= \sum_{k=1}^K \sum_{v=1}^V \left( \log \frac{\sqrt{\gamma_1}}{\sqrt{NN^{\tilde{\sigma}}(\tilde{\mathbf{W}})_{k,v}}} + \frac{NN^{\tilde{\sigma}}(\tilde{\mathbf{W}})_{k,v} + (NN^{\tilde{\mu}}(\tilde{\mathbf{W}})_{k,v} - B_{k,v}^R)^2}{2\gamma_1} - \frac{1}{2} \right) \quad (26)
\end{aligned}$$

As the elements of the same topic sum up to one, a normalization step follows.

A similar computation process applies to  $\text{KL}(q_{\psi}(\boldsymbol{\phi}^R) \| p(\boldsymbol{\phi}^R))$ . The variational distribution is  $\text{LogNormal}(NN^{\mu}(\mathbf{W})_{k,v}, NN^{\sigma}(\mathbf{W})_{k,v})$ , while the prior is  $\text{LogNormal}(B_{k,v}^R, \gamma_2)$ . We set  $B_{k,v}^R$  as 0 and  $\gamma_2$  as  $(VK - 1)/(VK)$ . The KL divergence is computed similarly to Equation (26).

For the fourth term  $\text{KL}(q_{\psi}(\boldsymbol{\phi}^S) \| p(\boldsymbol{\phi}^S))$ ,  $\boldsymbol{\phi}^S$  is conditionally independent of  $\mathbf{F}^I, \mathbf{F}^M, \mathbf{F}^A$ , and  $\mathbf{Y}$  given  $\tilde{\mathbf{W}}$  and  $\mathbf{W}$ . Hence, the inference network takes  $\tilde{\mathbf{W}}$  and  $\mathbf{W}$  as the input to obtain the variational distribution  $\text{LogNormal}(NN^{s1}(\tilde{\mathbf{W}}, \mathbf{W})_{k,v}, NN^{s2}(\tilde{\mathbf{W}}, \mathbf{W})_{k,v})$ . The prior distribution is  $\text{LogNormal}(B_{k,v}^S, \gamma_3)$ . We set  $B_{k,v}^S$  as 0 and  $\gamma_3$  as  $(UK - 1)/(UK)$ . The KL divergence is computed similarly.

In this way, we can compute the all the KL divergence terms in Equation (19) in close forms.

### Learning Parameters of Networks

We have defined multiple inference networks for the variational distributions, including  $N^{\text{mean}}$ ,  $NN^{\text{std}}$ ,  $NN^{\tilde{\delta}_1}$ ,  $NN^{\tilde{\delta}_2}$ ,  $NN^{\delta_1}$ ,  $NN^{\delta_2}$ ,  $NN^{\tilde{\mu}}$ ,  $NN^{\tilde{\sigma}}$ ,  $NN^{\mu}$ ,  $NN^{\sigma}$ ,  $NN^{s1}$ , and  $NN^{s2}$ . Their architectural details are shown in Appendix 5. The classic Expectation Maximization (EM) algorithm is adopted for learning their parameters together with the networks introduced in the generative process i.e.,  $NN^L$ ,  $NN^I$ ,  $NN^M$ , and  $NN^A$ . Particularly, in the E-step, from these inference networks, we obtain samples of hidden variables including  $\boldsymbol{\theta}$ ,  $\tilde{\boldsymbol{\pi}}$ ,  $\tilde{\boldsymbol{\phi}}^R$ ,  $\boldsymbol{\phi}^S$ ,  $\boldsymbol{\pi}$ , and  $\boldsymbol{\phi}^R$  to estimate the lower bound of the first term in Equation (13). We also compute the KL divergence for the second term of Equation (13). In this way, we estimate the lower bound of ELBO and then

maximize it by learning the parameters of the inference networks. The parameters of networks in the generative process are fixed in the E-step but are updated in the M-step to maximize the lower bound of the ELBO. The inference networks are fixed in the M-step. We iterate between the E-step and the M-step until convergence. Common training methods such as the Adam optimizer can be introduced for both the E-step and the M-step.

### Training Incomplete Topic Inference Networks for New Videos

To predict a new video  $d$ , we aim to infer the topic  $\boldsymbol{\theta}_d$  and then make the prediction based on  $NN^L(\boldsymbol{\theta}_d)$ . However, a new video does not have the ground truth label  $y_d$ , which is required by the previous topic inference network as shown in Equations (21) and (22). Moreover, a new video can have two scenarios: with a transcript and without a transcript. The second scenario is especially common on short-form video platforms, because many videos do not have narratives and use background music as a template instead. The inputs of videos with transcripts include  $\tilde{\mathbf{w}}_d, \mathbf{f}_d^I, \mathbf{f}_d^M$ , and  $\mathbf{f}_d^A$ . The inputs of videos without transcript include  $\mathbf{f}_d^I, \mathbf{f}_d^M$ , and  $\mathbf{f}_d^A$ . To resolve the incomplete information, they need incomplete topic inference networks. Formally, for videos with transcripts, the incomplete topic inference network is designed as:

$$\boldsymbol{\mu}'_d = NN^{\text{Incomplete}1}(\tilde{\mathbf{w}}_d, \mathbf{f}_d^I, \mathbf{f}_d^M, \mathbf{f}_d^A); \boldsymbol{\sigma}'_d = NN^{\text{Incomplete}2}(\tilde{\mathbf{w}}_d, \mathbf{f}_d^I, \mathbf{f}_d^M, \mathbf{f}_d^A) \quad (27)$$

For videos without transcripts, the incomplete inference network is designed as:

$$\boldsymbol{\mu}'_d = NN^{\text{Incomplete}3}(\mathbf{f}_d^I, \mathbf{f}_d^M, \mathbf{f}_d^A); \boldsymbol{\sigma}'_d = NN^{\text{Incomplete}4}(\mathbf{f}_d^I, \mathbf{f}_d^M, \mathbf{f}_d^A) \quad (28)$$

The architectural details of the incomplete inference networks are shown in Appendix 5. For both scenarios, we draw a sample of  $\mathbf{r}_d$  from  $\mathcal{N}(\boldsymbol{\mu}'_d, \text{diag}(\boldsymbol{\sigma}'_d^2))$  and obtain  $\boldsymbol{\theta}_d$  by softmax. The previously trained topic inference network (i.e.,  $NN^{\text{mean}}$  and  $NN^{\text{std}}$ ) is utilized to guide the training of the incomplete networks. We denote the distribution of  $\mathbf{r}_d$  from the incomplete inference network (i.e., Equations (27) or (28)) as  $q'_{\Psi}(\mathbf{r}_d)$ . This distribution should be close to the

distribution from the complete inference network, i.e.,  $q_{\Psi}(\mathbf{r}_d)$ . Hence, we initialize the incomplete inference networks with the complete one and then fine-tune it to reduce the KL divergence, i.e.,  $\text{KL}(\mathcal{N}(\boldsymbol{\mu}_d, \text{diag}(\boldsymbol{\sigma}_d^2)) \parallel \mathcal{N}(\boldsymbol{\mu}'_d, \text{diag}(\boldsymbol{\sigma}'_d^2)))$ .

### Depressive Impact Prediction on New Videos

The trained incomplete topic inference networks are utilized to predict the depressive impact of new videos. We feed video's information into the model to obtain the topics  $\boldsymbol{\theta}_d$ , and then make predictions using  $NN^L(\boldsymbol{\theta}_d)$ . We do not sample  $\mathbf{r}_d$ , but use the expectation  $\boldsymbol{\mu}_d$  to represent  $\mathbf{r}_d$  to generate  $\boldsymbol{\theta}_d$ . This helps to reduce the randomness for prediction, thus improving performance.

## EMPIRICAL ANALYSES

### Data Collection and Preparation

We collect data from Douyin (TikTok in China) and TikTok, which are the most popular short-form video platforms. Since collecting the entire videos on these platforms is infeasible, we select a subset that has the highest priority to the platforms as our testbed. Among the videos on these platforms, the ones related to sadness concern experts, parents, media, and policymakers the most. Not all the “sadness” videos result in a depressive impact on viewers, as some are encouraging and positive videos about recovering from past sadness. A group of videos can indeed induce depressive moods for viewers, and some have a higher depressive impact than others. Platforms are eager to know the depressive impact of any new videos about sadness so that the platforms can tune their recommendation algorithms for these videos. Specifically, once our model predicts the depressive impact risk of new videos, those with a high predicted depressive impact should be recommended less to viewers compared to those with a low predicted depressive impact. In addition, our model uncovers the specific and more nuanced topics – such as domestic violence experiences, child abuse stories, and trauma events – under the general sadness umbrella. According to viewers' personal experience and personality, different

viewers perceive those different topics distinctively. A once-abused viewer may find child abuse stories more depressive than other topics, while a viewer in grief may find trauma events more depressive than others. These topics can be disclosed in the corresponding videos so that viewers can choose whether and what to watch to be fully aware of the potential depressive impact uniquely to them.

Table 1. Summary Statistics of Datasets		
Statistics	Douyin	TikTok
Language	Chinese	English
No. of Videos	871	1,396
No. of Comments	76,545	165,299
Avg. Duration Per Video (s)	56.4	22.3
Avg. No. of Comments Per Video	87.9	118.4
Avg. No. of Words Per Comment	10.3	8.3
No. of Unique Users	69,772	150,886
No. of Depressive Videos	420	654
No. of Non-Depressive Videos	431	742

For the Douyin dataset, we collect all the resulting videos from a search using keywords: “anxious,” “unemployed,” “pass away,” “depression disorder,” “depressed,” “sad,” “sorrow,” “grief,” and “breakup.” These keywords are translated into Chinese. For the TikTok dataset, we collect all the resulting videos from a search using keywords: “sad,” “mood,” “broken heart,” and “heartbroken.” To clarify, these keywords are not the topics related to the depressive impact that our model aims to learn. On one hand, for the videos in the search results, they simply suggest that at least one keyword appears in the title or description of the video, which is written by *video creators*. They are not a measurement or direct reflection of the topics related to *viewers*’ perceived depressive impact, which necessitates supervision of the viewers’ comments. The nuanced topics within the video content that truly relate to depressive impact may also diverge from keywords in its title and description. On the other hand, as mentioned above, not all videos from this keyword search result in a depressive impact on viewers because some are positive videos to reflect on past experiences. Besides, every video’s degree of depressive impact is

drastically different, which demands our model’s prediction. Table 1 shows the summary statistics of the two datasets. To show our method’s generalizability in videos in other categories, i.e., without sadness-related keywords, we will further verify our method’s robustness in general-topic videos (search using neutral keywords) by the end of the empirical analyses (Table 10).

As mentioned in the introduction, a video’s depressive impact on viewers can be observed by the proportion of depressive comments of the video. Accordingly, we need to label whether a comment shows depressive moods for model training purposes. To clarify, this is not to label the clinical depression diagnosis of the viewer. As defined in the introduction, the depressive impact prediction aims to reduce the negative mental impact on viewers when they watch videos, which aligns with the concerns of platforms, mainstream media, experts, and parents. Clinical depression diagnosis, however, is the determination of a disease that is privately assessed at the doctor’s office. Videos with depressive impacts may increase the risk of major depression disorder (MDD) but are not equivalent to MDD diagnosis. Nevertheless, videos identified with a depressive impact deserve much-needed interventions from platforms, such as recommendation algorithm revision and viewer discretion, which alleviate pressing criticisms from society. To assess whether a comment is a depressive comment, we leverage large language models (LLMs), as they have outperformed many models trained on various datasets and have been frequently used to alleviate the need for task-specific data annotations (Yu et al. 2023). In this work, we select a freely accessible LLM, ChatGLM2-6B, that is most suited for Chinese and English corpora. ChatGLM2-6B contains 6.2 billion parameters. It is optimized for Chinese and English dialogues. Other free LLMs, such as Llama2, have restrictions on classifying depressive texts, and thus cannot generate a response about depressive labels. To validate the accuracy of the LLM-generated labels, we randomly select 100 comments from each dataset and leverage two expert annotators with a bioinformatics and mental health research background to label them as

depressive or non-depressive. One expert labeled all the 200 comments, and the other expert verified the resulting annotation. Using the experts' labels as the ground truth, the accuracy of the Douyin data annotation is 96%, and the accuracy of the TikTok data annotation is 94%, both achieving high performance.

To classify videos into depressive and non-depressive, we need to determine the proportion of depressive comments as the positive-negative sample cutoff. That is, videos whose proportion of depressive comments is higher than the cutoff are classified as depressive-impacting videos (positive samples) in the training data. We pivot away from directly using the proportion of depressive comments as the outcome variable to formulate it as a regression problem. This is because when our model is implemented by platforms, they would need to only identify a group of videos with high depressive impacts to display viewer discretion about depressive topics, rather than adding viewer discretion to all videos – videos without depressive content do not have depressive topics either. Such a group division naturally necessitates a classification model rather than a regression model. It is also difficult for a regression model to trace back the topics associated with the prediction of a particular class. The cutoff of the proportion of depressive comments highly relies on the end users' needs. For instance, videos with more than 5% depressive comments could be alarming for some platforms, while other platforms may be willing to tolerate 10% depressive comments. For demonstration purposes, we choose the proportion of depressive comments that can make balanced depressive and non-depressive video samples. To show that our model is robust and accurate in different cutoffs and in imbalanced predictions, we will experiment with various proportions of depressive comments as the classification cutoff by the end of the empirical analyses (Table 9).

### **Depression Ontology Evaluation**

As described in the literature review, we construct a depression ontology as the medical

knowledge base, consisting of three categories of external and environmental factors: sharing depressive symptom experiences, sharing major life event stories, and sharing ongoing treatment experiences. Each category includes a list of specific depressive factors (e.g., violence, abuse, and body shaming) adopted from the medical studies. These factors serve as the seed words for our model. To validate this ontology, we engage a panel of medical experts. Two psychiatrists from a nationally recognized hospital were invited to evaluate our depression ontology. Following their initial independent reviews, the psychiatrists convened to include entities that were absent in the initial version while eliminating redundant and clinically irrelevant entities. The final ontology encompassing 244 factors, approved by the medical expert panel, is employed in our study.

To further evaluate the quality of the ontology, we adapt previous work in ontology evaluation (Ouyang et al. 2011) and measure the coverage of the ontology by comparing the number of concepts in the ontology with regard to multiple widely used depression diagnosis scales, including DSM-5-TR Self-Rated Level 1 Cross-Cutting Symptom Measure – Adult (DSM-5-TR) (APA 2022), Patient Health Questionnaire (PHQ-9) (Martin et al. 2006), and Quick Inventory of Depressive Symptomatology-Self-Report (QIDS-SR) (Rush et al. 2003).

Specifically, we define  $C = \{c_1, c_2, \dots, c_i, \dots, c_n\}$  as the set of  $n$  concepts in the depression ontology  $O$ . Let  $T = \{t_1, t_2, \dots, t_j, \dots, t_m\}$  be the set of  $m$  medical terminologies in the depression diagnosis criteria  $D$ . The coverage of  $O$  to  $D$  is calculated as  $\frac{\sum_{c \in C(O)} \sum_{t \in T} I(c, t)}{m}$ . If there is a  $t$  or synonyms in  $\{c_1, c_2, \dots, c_n\}$ , we set  $I(c, t) = 1$ ; otherwise,  $I(c, t) = 0$ . The resulting coverages of our depression ontology to DSM-5-TR, PHQ-9, and QIDS-SR are presented in Table 2.

Table 2. The Coverage Rate of Depression Ontology to Depression Diagnosis Scales

Depression Diagnosis Scales	DSM-5-TR	PHQ-9	QIDS-SR
Coverage Rate	85.6%	95.2%	93.8%

Overall, the coverage calculation results demonstrate that our ontology can comprehensively

cover the widely used depression scales.

### **Prediction Evaluations**

According to our literature review, we select four groups of baseline models. The first group is the commonly adopted machine learning methods in social media-based depression prediction, including K-Nearest Neighbor (KNN), Random Forest (RF), AdaBoost, XGBoost, and Support Vector Machine (SVM). These studies and our study have closely related research contexts (social media and mental health). However, these methods are not able to identify the topics related to depressive impacts. Relatedly, the second group is the deep learning methods in social media-based depression prediction applicable to our study, including 3DCNN, CNN, and RNN. Since our proposed method is based upon the topic modeling approach, the third group pertains to the topic models adopted in social media-based depression prediction as well as other common topic models, including LDA, seeded LDA, SLDA, ETM, WLDA, and Scholar. The fourth group is the state-of-the-art video-based depression prediction studies that are applicable to our study, including Yang et al. (2016), Yang et al. (2017), and Ray et al. (2019). These studies and our study address a similar mental health context and deal with similar data modalities (videos). We adopt F1-score, precision, and recall as the evaluation metrics. The best model should have the highest F1-score. All the baseline models and our model are fine-tuned via large-scale experiments to reflect their best performance capability in our problem context. The following performances are the mean of 10 random experimental runs. We also report the standard deviations of the performances to show the statistical significance.

We first compare with machine learning methods in social media-based depression prediction. To ensure a fair comparison, the input features to the machine learning models are the learned representations from 3DCNN. This is because they are more effective than manually engineered features, and crafted textual features in the literature are not obtainable for video data. As reported

in Table 3, compared with machine learning methods, our proposed method outperforms all the baseline models. Our leading result is consistent in both the Douyin and TikTok datasets. In the Douyin dataset, we outperform the best machine learning method (AdaBoost) in F1-score by 0.177. In the TikTok dataset, our method outperforms the best machine learning method (XGBoost) in F1-score by 0.136. These machine learning methods are not able to learn the topics related to depressive impacts.

Table 3. Comparison with Machine Learning Methods

Method	Statistics	Douyin			TikTok		
		F1	Precision	Recall	F1	Precision	Recall
Ours	Mean	<b>0.782</b>	<b>0.777</b>	<b>0.787</b>	<b>0.835</b>	<b>0.815</b>	<b>0.857</b>
	STD	0.010	0.007	0.014	0.010	0.023	0.015
KNN	Mean	0.553	0.570	0.568	0.627	0.616	0.639
	STD	0.051	0.081	0.084	0.023	0.029	0.026
RF	Mean	0.543	0.598	0.500	0.645	0.643	0.653
	STD	0.047	0.074	0.052	0.036	0.057	0.066
AdaBoost	Mean	0.605	0.623	0.623	0.643	0.646	0.643
	STD	0.033	0.051	0.017	0.045	0.039	0.062
XGBoost	Mean	0.548	0.583	0.525	0.699	0.655	0.752
	STD	0.055	0.050	0.047	0.041	0.045	0.060
SVM	Mean	0.548	0.573	0.525	0.625	0.611	0.640
	STD	0.031	0.046	0.037	0.040	0.047	0.040

Table 4. Comparison with Deep Learning Methods

Method	Statistics	Douyin			TikTok		
		F1	Precision	Recall	F1	Precision	Recall
Ours	Mean	<b>0.782</b>	<b>0.777</b>	<b>0.787</b>	<b>0.835</b>	<b>0.815</b>	<b>0.857</b>
	STD	0.010	0.007	0.014	0.010	0.023	0.015
3DCNN	Mean	0.630	0.575	0.698	0.702	0.749	0.660
	STD	0.018	0.019	0.022	0.014	0.006	0.029
CNN	Mean	0.578	0.536	0.628	0.619	0.664	0.580
	STD	0.036	0.029	0.064	0.015	0.016	0.017
RNN	Mean	0.578	0.550	0.618	0.631	0.676	0.596
	STD	0.046	0.032	0.114	0.005	0.006	0.002

We then compare with deep learning methods in social media-based depression prediction. Table 4 suggests that our method outperforms all the deep learning methods in both datasets. In the Douyin dataset, our method observes a leap of 0.152 in F1-score, compared to the best-performing benchmark (3DCNN). In the TikTok dataset, we outperform 3DCNN in F1-score by

0.133. This improvement is partially driven by our method’s ability to learn depressive topics.

Next, we compare with topic models in social media-based depression prediction as well as other common topic models, encompassing both LDA-based models and NTM-based models, as well as non-seeded topic models and seeded topic models. As shown in Table 5, our method outperforms all the benchmark topic models. In the Douyin dataset, our method outperforms the best topic model (WLDA) in F1-score by 0.027. In the TikTok dataset, we outperform the best topic model (Scholar) in F1-score by 0.032. It is worth noting that the topic models generally achieve better performances than machine and deep learning-based methods in our context. This is because the topic models leverage the learned topics to make the prediction, which is more relevant to the depressive risk factors. Noisy information is filtered out in the topic modeling approaches. Whereas in machine and deep learning models, all video information, regardless of its depressive impact relevance, is encoded into the input feature.

Table 5. Comparison with Topic Models

Method	Statistics	Douyin			TikTok		
		F1	Precision	Recall	F1	Precision	Recall
<b>Ours</b>	Mean	<b>0.782</b>	<b>0.777</b>	<b>0.787</b>	<b>0.835</b>	<b>0.815</b>	<b>0.857</b>
	STD	0.010	0.007	0.014	0.010	0.023	0.015
LDA	Mean	0.735	0.731	0.739	0.743	0.751	0.736
	STD	0.005	0.011	0.017	0.019	0.017	0.022
SeededLDA	Mean	0.743	0.722	0.766	0.788	0.771	0.807
	STD	0.014	0.006	0.023	0.009	0.015	0.019
SLDA	Mean	0.745	0.744	0.746	0.789	0.775	0.805
	STD	0.007	0.007	0.020	0.007	0.018	0.011
ETM	Mean	0.737	0.742	0.732	0.791	0.768	0.816
	STD	0.012	0.014	0.014	0.022	0.039	0.015
WLDA	Mean	0.755	0.736	0.775	0.799	0.796	0.803
	STD	0.011	0.010	0.017	0.014	0.006	0.026
Scholar	Mean	0.727	0.740	0.714	0.803	0.775	0.834
	STD	0.006	0.016	0.007	0.007	0.007	0.009

The topics learned by the above topic models can explain the factors contributing to the prediction result. In Table 6, we show the quality of the topics learned by these models, using the widely adopted topic coherence metric. It assesses how well a topic is supported by a text set. The

higher the topic coherence, the better quality the topics are. We report the topic coherence of the top 10 words and the top 20 words. The results indicate that our method can learn the best-quality topics among all the topic models, which is consistent in both datasets. We will showcase the specific topics that our method learned in the next subsection.

Table 6. Evaluation of Topic Quality

Method	Statistics	Douyin		TikTok	
		Coherence Top-10	Coherence Top-20	Coherence Top-10	Coherence Top-20
<b>Ours</b>	Mean	<b>-0.907</b>	<b>-1.074</b>	<b>-1.325</b>	<b>-1.572</b>
	STD	0.090	0.068	0.145	0.111
LDA	Mean	-4.001	-4.373	-4.614	-5.395
	STD	0.222	0.168	0.097	0.041
SeededLDA	Mean	-1.815	-1.987	-6.648	-7.847
	STD	0.083	0.039	0.109	0.106
SLDA	Mean	-2.770	-3.443	-2.979	-3.236
	STD	0.214	0.211	0.156	0.109
ETM	Mean	-1.832	-1.968	-1.832	-2.086
	STD	0.154	0.120	0.161	0.198
WLDA	Mean	-1.733	-2.212	-1.938	-2.373
	STD	0.181	0.203	0.232	0.161
Scholar	Mean	-1.414	-2.853	-1.989	-2.626
	STD	0.440	0.324	0.244	0.208

Table 7. Comparison with Video-based Depression Prediction Studies

Method	Statistics	Douyin			TikTok		
		F1	Precision	Recall	F1	Precision	Recall
<b>Ours</b>	Mean	<b>0.782</b>	<b>0.777</b>	<b>0.787</b>	<b>0.835</b>	<b>0.815</b>	<b>0.857</b>
	STD	0.010	0.007	0.014	0.010	0.023	0.015
Yang et al. (2016)	Mean	0.527	0.550	0.533	0.606	0.575	0.643
	STD	0.058	0.010	0.072	0.027	0.024	0.053
Yang et al. (2017)	Mean	0.577	0.578	0.578	0.650	0.647	0.654
	STD	0.018	0.033	0.033	0.006	0.019	0.008
Ray et al. (2019)	Mean	0.582	0.546	0.630	0.652	0.666	0.642
	STD	0.031	0.011	0.041	0.018	0.032	0.049

Lastly, we compare with video-based depression prediction studies. As reported in Table 7, our method significantly outperforms them in both datasets. In the Douyin dataset, we improve the F1-score of the best-performing video-based depression prediction model (Ray et al. 2019) by 0.200. In the TikTok dataset, our F1-score improvement over Ray et al. (2019) is 0.183. These studies have similar data modalities to our study. However, their primary prediction goal is not

videos' depressive impacts but rather users' depression status. Such a misalignment could partially contribute to their under-performing results in our problem.

Since our model is composed of multiple novel designs, we conduct four ablation studies, each removing one design from the full model to test its effectiveness. Each of these designs pertains to one of our methodological novelties. The first ablation removes the design of multi-origin topics (video topics and comment topics), and only reserves the generative process from video topics. The second ablation removes the design of two sets of topics (seed topics and regular topics) and only reserves the seed topics. This will result in the model being unable to discover new topics in the social media context. The third ablation removes the auto-supervision capability. Consequently, the model loses the ability to automatically learn the optimal level of supervision from seed words. The fourth ablation removes the pre-trained generative process. This component is designed to encourage the model to converge to optimal minimal. As reported in Table 8, removing any design will significantly hamper the model performance. This result is also consistent in both the Douyin dataset and TikTok dataset. This suggests that our design choice is optimal, and our methodological novelties are empirically effective. In the next subsection, we will further visualize our novelty about automatically discovering depressive topics related to the existing knowledge base as well as exploring from new social media context.

Table 8. Ablation Studies

Method	Statistics	Douyin			TikTok		
		F1	Precision	Recall	F1	Precision	Recall
<b>Ours</b>	Mean	<b>0.782</b>	<b>0.777</b>	<b>0.787</b>	<b>0.835</b>	<b>0.815</b>	<b>0.857</b>
	STD	0.010	0.007	0.014	0.010	0.023	0.015
Without Multi-origin	Mean	0.697	0.652	0.747	0.756	0.752	0.760
	STD	0.008	0.009	0.013	0.018	0.011	0.028
Without Two Sets of Topics	Mean	0.705	0.694	0.716	0.785	0.764	0.808
	STD	0.007	0.016	0.021	0.004	0.007	0.009
Without Auto-supervision	Mean	0.738	0.734	0.743	0.798	0.790	0.806
	STD	0.021	0.022	0.029	0.023	0.021	0.037
Without Pre-trained Generative Process	Mean	0.750	0.753	0.747	0.813	0.768	0.863
	STD	0.008	0.012	0.015	0.009	0.003	0.015

As discussed above, the choice of depressive comment proportions as the classification cutoff is highly dependent on the end users' needs. In Table 9, we report the results of different depressive comment proportions as the cutoff. For instance, a 5% cutoff indicates that videos with more than 5% depressive comments are classified as depressive-impacting videos in the training data. The results suggest that our method is able to achieve robust and consistently high performance in any cutoffs. This result is also consistent in both datasets. Therefore, platforms with low depressive impact tolerance (e.g., 5%) and platforms with high depressive impact tolerance (e.g., 10% and higher) can both benefit from using our method.

Table 9. Analysis of Different Depressive Comment Proportions

Depressive Comment Proportion	Statistics	Douyin			TikTok		
		F1	Precision	Recall	F1	Precision	Recall
5%	Mean	0.782	0.777	0.787	0.834	0.835	0.834
	STD	0.010	0.007	0.014	0.008	0.028	0.012
10%	Mean	0.774	0.763	0.788	0.835	0.815	0.857
	STD	0.016	0.019	0.039	0.010	0.023	0.015
20%	Mean	0.797	0.768	0.830	0.852	0.827	0.878
	STD	0.008	0.019	0.020	0.012	0.018	0.009
30%	Mean	0.756	0.740	0.774	0.858	0.841	0.877
	STD	0.018	0.034	0.005	0.019	0.015	0.035

Table 10. Evaluation in General-Topic Videos

Dataset	Statistics	Douyin			TikTok		
		F1	Precision	Recall	F1	Precision	Recall
Sadness	Mean	0.782	0.777	0.787	0.835	0.815	0.857
	STD	0.010	0.007	0.014	0.010	0.023	0.015
General	Mean	0.765	0.752	0.780	0.819	0.797	0.841
	STD	0.009	0.018	0.006	0.016	0.012	0.022

As discussed in Data Collection and Preparation, we select the videos with the highest priority as the testbed, as it is infeasible to collect all videos. The keywords for selecting these videos are sadness-related. To show that our method can accurately identify depressive-impacting videos from general videos, we further collect 500 videos each from the Douyin dataset and TikTok dataset. The keywords for selecting these additional videos are neutral words and are not related to sadness. The keywords used in the Douyin dataset include: "life," "health," "relation,"

“music,” “work,” and “graduation.” The keywords used in the TikTok dataset include: “health,” “emotion,” and “life.” Table 10 shows that our method reaches consistently high performance in both the sadness-related videos and general-topic videos, which holds in both datasets.

### **Explainable Insights about the Learned Topics**

Our proposed method is able to discover topics related to depressive impacts and leverage them to make the prediction. The learned topics offer explainable insights about our predictions. In Figure 3, we showcase three randomly selected videos that are predicted to have a depressive impact. We visualize the learned topic distributions and representative topics. The learned topics of Video 1 suggest this video is about stories of depression and PTSD. The content creator also mentioned suicidal thoughts in the video. As a result, our model predicts this video as depressive-impacting. Video 2’s topics are related to divorce, fighting with her husband, and disappointment. These experiences have negative effects on the viewers’ mental state as well. Video 3 contains topics about unemployment, family separation, and even suicidal thoughts. These topics led our model to classify this video as depressive impacting.

Some of the learned topics are influenced by the seed words from the existing medical ontology, while others relate more to the social media context. One nice property of our method is that it can inform the weight of the seed topic for each learned topic, so that we know the degree of influence or relevance of the medical ontology on the learned topics. In the middle tables in Figure 3, the “Seed Topic Weight” column indicates the weight of the seed topic for each learned topic. The higher the weight, the more this topic is related to the existing medical ontology. For instance, Topic 1 (top words: suicide, punishment, blame, failure, panic, death, failure) in Video 1 is highly related to the medical ontology. This topic corresponds to the entity “thoughts of suicide” in the medical ontology. Topic 2 (top words: violence, emotional, abuse, loss) in Video 2 is closely related to the medical ontology too. This topic corresponds to the entity “history of

violence" in the medical ontology. Topic 1 (top words: mood, suicide, depression, pain, spirit, symptom, mood) in Video 3 is also highly related to the medical ontology. This topic corresponds to the entity "thoughts of suicide" in the medical ontology.

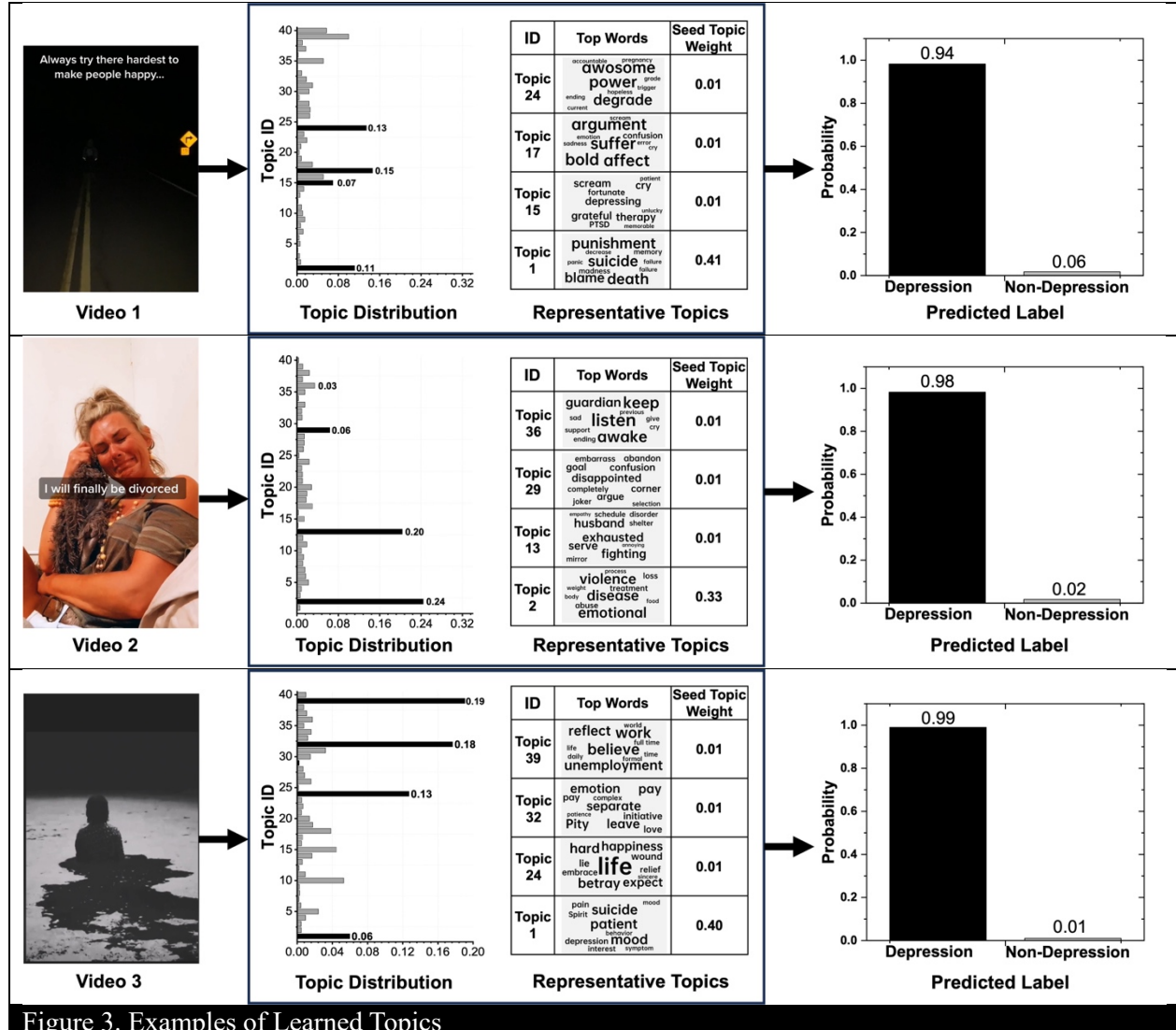


Figure 3. Examples of Learned Topics

## DISCUSSION AND CONCLUSION

While short-form videos offer a transformational medium for entertainment and social networking in recent years, their mental impact on viewers deserves careful investigation. In particular, predicting short-form videos' depressive impact on viewers is especially critical to minimize widespread negative mental influences. Positioned in the computational design science

paradigm in IS, we propose a novel Knowledge-guided Multimodal Neural Topic Model for this prediction, while addressing the technical challenges of single-origin topics, unknown topic sources, unclear seed supervision, and suboptimal convergence. We perform comprehensive empirical analyses on two datasets to compare our proposed method and the state-of-the-art benchmarks, which prove our method's superiority in this context.

### **Implications to the IS Knowledge Base**

Our work belongs to the computational design science research in IS, which develops computational methods to solve business and societal problems and aims to make methodological contributions (Padmanabhan et al. 2022; Rai 2017; Simchi-Levi 2020). In this regard, our proposed Knowledge-guided Multimodal NTM, the designed IT artifact, is a novel extension to seeded NTMs. To design our method, we overcome significant technical challenges. This design process reveals three general design principles that can be applied to other design science research in IS: 1) designing two sets of topic generative processes can complement mono-topic models in discovering new topics while adhering to the supervision of seed topics; 2) medical ontologies can function as seed words to offer medical knowledge supervision in machine learning models; 3) a pre-trained generative process can optimize the training process of NTMs.

### **Managerial and Practical Implications**

Our study offers managerial and practical implications for short-form video platforms and policymakers. Short-form video platforms are actively addressing society's concerns about their impact on viewers' mental health. Equipped with our model, these platforms can tackle this issue from two directions. Firstly, when a video is published, the platforms can use our model to predict a depressive-impacting score for this video. They can redesign their video recommendation algorithm to factor in this depressive-impacting score, such that highly depressive-impacting videos are not constantly recommended to the same user. Secondly, our method can explain the

topics contained in a video that are related to depression risk factors. The platforms can display viewer discretion as a banner below a video. This discretion could disclose the topics in the video that might result in depressive moods. This viewer discretion mechanism is frequently used by video platforms to warn users of potential discomfort or conflict of interest. For instance, YouTube shows viewer discretion when a video contains violent or bloody content and when a channel is sponsored by a government entity. Policymakers can use our model to scrutinize the status quo of the platforms' mental influence on users and use the results as evidence to back up their future policies.

### **Generalizability to Other IS Areas**

Our proposed method could be used in many other IS areas and offer managerial implications for predictive and prescriptive analytics in these areas. Over the years, design science methods that predict future actions (i.e., predictive analytics) or specify optimal decisions (i.e., prescriptive analytics) have been developed to solve problems in a diverse set of domains, such as social media user engagement, infodemic management, and video content management. Below we elaborate on how our proposed method can generate managerial insights for these areas.

**Social media user engagement:** IS studies find great interest in predicting users' engagement with social media videos (Liu et al. 2020; Xie et al. 2023). With pre-defined labels of user engagement, our model can be trained with the video-label pairs to predict a video's user engagement. Theories of social network analysis can serve as the knowledge guide and function as the seed words in our seeded neural topic model.

**Infodemic management:** An infodemic is too much information including false or misleading information in digital and physical environments during a disease outbreak. Infodemics frequently disseminate among short-form videos. Our model can be trained in the infodemic context with corresponding class labels. Existing knowledge of the factors of information

dissemination can guide the learning of topics related to infodemics.

Video content management: Short-form video platforms are concerned about violent videos.

Manual annotation can be employed to provide ground truth labels for violent content prediction.

Prior literature about the characteristics of violent content can provide domain knowledge into the learning of violent topics. In this sense, our model can be well suited for this task.

### **Limitations and Future Research**

This study has a few limitations. Firstly, this study aims to predict the depressive impact on viewers. However, the videos' impact on clinical major depression disorder is unknown. This is because users' clinical depression diagnosis is not observable, which often requires psychiatrists' assessment in the clinic. Nevertheless, our depressive impact prediction already offers fruitful implications on the platforms' end, whereas viewers' clinical depression diagnosis can be beneficial for intervention measures on viewers' end. If budget permits, future research can extend this study by following up with a group of users and obtaining their clinical depression diagnosis. Secondly, our method focuses on videos. However, other social media forms, such as stories on Twitter (texts) and Instagram (images), can cause a depressive impact on users as well. Future research can adapt our method and revise the data representation to accommodate other data formats.

### **REFERENCES**

APA. 2022. *DSM-5-TR(Tm) Classification*, American Psychiatric Association Publishing.

Arsene, O., I. Dumitache, and I. Mihu. 2011, "Medicine Expert System Dynamic Bayesian Network and Ontology Based," *Expert Systems with Applications* (38:12), pp. 15253-15261.

Bardhan, I., J. Oh, Z. Zheng, and K. Kirksey. 2015, "Predictive Analytics for Readmission of Patients with Congestive Heart Failure," *Information Systems Research* (26:1), pp. 19-39.

Beck, A. T., and B. A. Alford. 2009. *Depression: Causes and Treatment*, University of Pennsylvania Press.

Ben-Assuli, O., and R. Padman. 2020, "Trajectories of Repeated Readmissions of Chronic Disease Patients: Risk Stratification, Profiling, and Prediction." *MIS Quarterly* (44:1), .

Bucur, A., I. R. Podină, and L. P. Dinu. 2021, "A Psychologically Informed Part-of-Speech Analysis of Depression in Social Media," *arXiv Preprint arXiv:2108.00279*.

Cao, Z., S. Li, Y. Liu, W. Li, and H. Ji. 2015. "A Novel Neural Topic Model and its Supervised Extension," *Proceedings of the AAAI Conference on Artificial Intelligence* (29:1), .

Card, D., C. Tan, and N. A. Smith. 2018. "Neural Models for Documents with Metadata," pp. 2031-2040.

Carpenter, A. 2023, "Associations between TikTok use, Mental Health, and Body Image among College Students," *Honors Theses*.

Chai, Y., Y. Liu, W. Li, B. Zhu, H. Liu, and Y. Jiang. 2024, "An Interpretable Wide and Deep Model for Online Disinformation Detection," *Expert Systems with Applications* (237:pp. 121588.

Chang, Y., W. Hung, and T. Juang. 2013. "Depression Diagnosis Based on Ontologies and Bayesian Networks," *2013 IEEE International Conference on Systems, Man, and Cybernetics*pp. 3452-3457.

Chao, M., J. Lei, R. He, Y. Jiang, and H. Yang. 2023, "TikTok use and Psychosocial Factors among Adolescents: Comparisons of Non-Users, Moderate Users, and Addictive Users," *Psychiatry Research* (325:pp. 115247.

Cheng, H., S. Liu, W. Sun, and Q. Sun. 2023, "A Neural Topic Modeling Study Integrating SBERT and Data Augmentation," *Applied Sciences* (13:7), pp. 4595.

Cheng, J. C., and A. L. Chen. 2022, "Multimodal Time-Aware Attention Networks for Depression Detection," *Journal of Intelligent Information Systems* (59:2), pp. 319-339.

Fard, M. M., T. Thonet, and E. Gaussier. 2020. "Seed-Guided Deep Document Clustering," pp. 3-16.

Ghosh, S., and T. Anwar. 2021, "Depression Intensity Estimation Via Social Media: A Deep Learning Approach," *IEEE Transactions on Computational Social Systems* (8:6), pp. 1465-1474.

Guo, Y., J. Liu, L. Wang, W. Qin, S. Hao, and R. Hong. 2023, "A Prompt-Based Topic-Modeling Method for Depression Detection on Low-Resource Data," *IEEE Transactions on Computational Social Systems*.

Gupta, P., Y. Chaudhary, F. Buettner, and H. Schütze. 2019. "Document Informed Neural Autoregressive Topic Models with Distributional Prior," *Proceedings of the AAAI Conference on Artificial Intelligence* (33:01), pp. 6505-6512.

He, L., J. C. Chan, and Z. Wang. 2021, "Automatic Depression Recognition using CNN with Attention Mechanism from Videos," *Neurocomputing* (422:pp. 165-175.

Hedman, J., N. Srinivasan, and R. Lindgren. 2013. "Digital Traces of Information Systems: Sociomateriality made Researchable," pp. 1069.

Hennig, P., D. Stern, R. Herbrich, and T. Graepel. 2012. "Kernel Topic Models," pp. 511-519.

Iqbal, M. 2023. "TikTok Revenue and Usage Statistics (2023)," *Business of Apps*Oct 31, .

Jagarlamudi, J., H. Daumé III, and R. Udupa. 2012. "Incorporating Lexical Priors into Topic Models," pp. 204-213.

Jung, H., H. Park, and T. Song. 2017, "Ontology-Based Approach to Social Data Sentiment Analysis: Detection of Adolescent Depression Signals," *Journal of Medical Internet Research* (19:7), pp. e259.

Li, X., X. Zhang, J. Zhu, W. Mao, S. Sun, Z. Wang, C. Xia, and B. Hu. 2019, "Depression Recognition using Machine Learning Methods with Different Feature Generation Strategies," *Artificial Intelligence in Medicine* (99:pp. 101696.

Lin, L., X. Chen, Y. Shen, and L. Zhang. 2020, "Towards Automatic Depression Detection: A BiLSTM/1D CNN-Based Model," *Applied Sciences* (10:23), pp. 8701.

Lin, Y., X. Gao, X. Chu, Y. Wang, J. Zhao, and C. Chen. 2023. "Enhancing Neural Topic Model

with Multi-Level Supervisions from Seed Words," *Findings of the Association for Computational Linguistics: ACL 2023*pp. 13361-13377.

Liu, D., X. L. Feng, F. Ahmed, M. Shahid, and J. Guo. 2022, "Detecting and Measuring Depression on Social Media using a Machine Learning Approach: Systematic Review," *JMIR Mental Health* (9:3), pp. e27244.

Liu, X., B. Zhang, A. Susarla, and R. Padman. 2020, "Go to You Tube and Call Me in the Morning: Use of Social Media for Chronic Conditions," *Management Information Systems Quarterly* (44:1), pp. 257-283.

Martin, A., W. Rief, A. Klaiberg, and E. Braehler. 2006, "Validity of the Brief Patient Health Questionnaire Mood Scale (PHQ-9) in the General Population," *General Hospital Psychiatry* (28:1), pp. 71-77.

Meyer, G., G. Adomavicius, P. E. Johnson, M. Elidrisi, W. A. Rush, J. M. Sperl-Hillen, and P. J. O'Connor. 2014, "A Machine Learning Approach to Improving Dynamic Decision Making," *Information Systems Research* (25:2), pp. 239-263.

Milton, A., L. Ajmani, M. A. DeVito, and S. Chancellor. 2023. "'I See Me here": Mental Health Content, Community, and Algorithmic Curation on TikTok," pp. 1-17.

Moreno, J. 2021. "TikTok Surpasses Google, Facebook as World's most Popular Web Domain," *Forbes*Dec 29, .

Ouyang, L., B. Zou, M. Qu, and C. Zhang. 2011. "A Method of Ontology Evaluation Based on Coverage, Cohesion and Coupling," (4:pp. 2451-2455.

Padmanabhan, B., N. Sahoo, and A. Burton-Jones. 2022, "Machine Learning in Information Systems Research," *Management Information Systems Quarterly* (46:1), pp. iii-xix.

Paul, K. 2022. "What TikTok does to Your Mental Health: 'It's Embarrassing we Know so Little'," *The Guardian*Oct 30, .

Pennebaker, J. W., M. E. Francis, and R. J. Booth. 2001, "Linguistic Inquiry and Word Count: LIWC 2001," *Mahway: Lawrence Erlbaum Associates* (71:2001), pp. 2001.

Pérez, A., J. Parapar, and Á Barreiro. 2022, "Automatic Depression Score Estimation with Word Embedding Models," *Artificial Intelligence in Medicine* (132:pp. 102380.

Perlis, R. H., J. Green, M. Simonson, K. Ognyanova, M. Santillana, J. Lin, A. Quintana, H. Chwe, J. Druckman, and D. Lazer. 2021, "Association between Social Media use and Self-Reported Symptoms of Depression in US Adults," *JAMA Network Open* (4:11), pp. e2136113.

Preidt, R. 2022. "Kids Who Witness Domestic Violence may Suffer Mentally for Decades," *HealthDay*Apr 27, .

Rai, A. 2017, "Editor's Comments: Diversity of Design Science Research," *MIS Quarterly* (41:1), pp. iii-xviii.

Ray, A., S. Kumar, R. Reddy, P. Mukherjee, and R. Garg. 2019. "Multi-Level Attention Network using Text, Audio and Video for Depression Prediction," pp. 81-88.

Rush, A. J., M. H. Trivedi, H. M. Ibrahim, T. J. Carmody, B. Arnow, D. N. Klein, J. C. Markowitz, P. T. Ninan, S. Kornstein, and R. Manber. 2003, "The 16-Item Quick Inventory of Depressive Symptomatology (QIDS), Clinician Rating (QIDS-C), and Self-Report (QIDS-SR): A Psychometric Evaluation in Patients with Chronic Major Depression," *Biological Psychiatry* (54:5), pp. 573-583.

Schlott, R. 2022. "How TikTok has Become a Dangerous Breeding Ground for Mental Disorders," *New York Post*Mar 12, .

Shmueli, G., and O. R. Koppius. 2011, "Predictive Analytics in Information Systems Research," *MIS Quarterly*pp. 553-572.

Simchi-Levi, D. 2020, "From the Editor: Diversity, Equity, and Inclusion in Management Science," *Management Science* (66:9), pp. 3802.

Smith, B. 2003. *Blackwell Guide to the Philosophy of Computing and Information*, Oxford: Blackwell.

Srivastava, A., and C. Sutton. 2016. "Autoencoding Variational Inference for Topic Models," *International Conference on Learning Representations*.

Tadesse, M. M., H. Lin, B. Xu, and L. Yang. 2019, "Detection of Depression-Related Posts in Reddit Social Media Forum," *Ieee Access* (7:pp. 44883-44893).

Toto, E., M. L. Tlachac, and E. A. Rundensteiner. 2021. "Audibert: A Deep Transfer Learning Multimodal Classification Framework for Depression Screening," *Proceedings of the 30th ACM International Conference on Information & Knowledge Management* pp. 4145-4154.

Wang, R., D. Zhou, and Y. He. 2019, "Atm: Adversarial-Neural Topic Model," *Information Processing & Management* (56:6), pp. 102098.

Wang, Y., Z. Wang, C. Li, Y. Zhang, and H. Wang. 2022, "Online Social Network Individual Depression Detection using a Multitask Heterogenous Modality Fusion Approach," *Information Sciences* (609:pp. 727-749).

Xie, J., Y. Chai, and X. Liu. 2023, "Unbox the Black-Box: Predict and Interpret YouTube Viewership using Deep Learning," *Journal of Management Information Systems* (40:2), pp. 541-579.

Xie, J., X. Liu, D. Dajun Zeng, and X. Fang. 2022, "Understanding Medication Nonadherence from Social Media: A Sentiment-Enriched Deep Learning Approach." *MIS Quarterly* (46:1), .

Yang, L., D. Jiang, L. He, E. Pei, M. C. Ovemeke, and H. Sahli. 2016. "Decision Tree Based Depression Classification from Audio Video and Language Information," *Proceedings of the 6th International Workshop on Audio/Visual Emotion Challenge* pp. 89-96.

Yang, L., H. Sahli, X. Xia, E. Pei, M. C. Ovemeke, and D. Jiang. 2017. "Hybrid Depression Classification and Estimation from Audio Video and Text Information," *Proceedings of the 7th Annual Workshop on Audio/Visual Emotion Challenge* pp. 45-51.

Yazdavar, A. H., H. S. Al-Olimat, M. Ebrahimi, G. Bajaj, T. Banerjee, K. Thirunarayan, J. Pathak, and A. Sheth. 2017. "Semi-Supervised Approach to Monitoring Clinical Depressive Symptoms in Social Media," pp. 1191-1198.

Yu, Y., Y. Zhuang, J. Zhang, Y. Meng, A. Ratner, R. Krishna, J. Shen, and C. Zhang. 2023. "Large Language Model as Attributed Training Data Generator: A Tale of Diversity and Bias," *Thirty-Seventh Conference on Neural Information Processing Systems*.

Zahra, M. F., T. A. Qazi, A. S. Ali, N. Hayat, and T. ul Hassan. 2022, "How TikTok Addiction Leads to Mental Health Illness? Examining the Mediating Role of Academic Performance using Structural Equation Modeling," *Journal of Positive School Psychology* (6:10), pp. 1490-1502.

Zhang, H., B. Chen, D. Guo, and M. Zhou. 2018. "WHAI: Weibull Hybrid Autoencoding Inference for Deep Topic Modeling," *International Conference on Learning Representations*.

Zhang, W., and S. Ram. 2020, "A Comprehensive Analysis of Triggers and Risk Factors for Asthma Based on Machine Learning and Large Heterogeneous Data Sources." *MIS Quarterly* (44:1), .

Zhang, X., S. Feng, R. Peng, and H. Li. 2022, "Using Structural Equation Modeling to Examine Pathways between Physical Activity and Sleep Quality among Chinese TikTok Users," *International Journal of Environmental Research and Public Health* (19:9), pp. 5142.

Zhao, H., D. Phung, V. Huynh, Y. Jin, L. Du, and W. Buntine. 2021. "Topic Modelling Meets Deep Neural Networks: A Survey," *Proceedings of the Thirtieth International Joint Conference on Artificial Intelligence (IJCAI-21)*.

Zheng, H., B. Kang, and H. Kim. 2007. "An Ontology-Based Bayesian Network Approach for Representing Uncertainty in Clinical Practice Guidelines," *Proceedings of the Third International Conference on Uncertainty Reasoning for the Semantic Web*pp. 85-96.

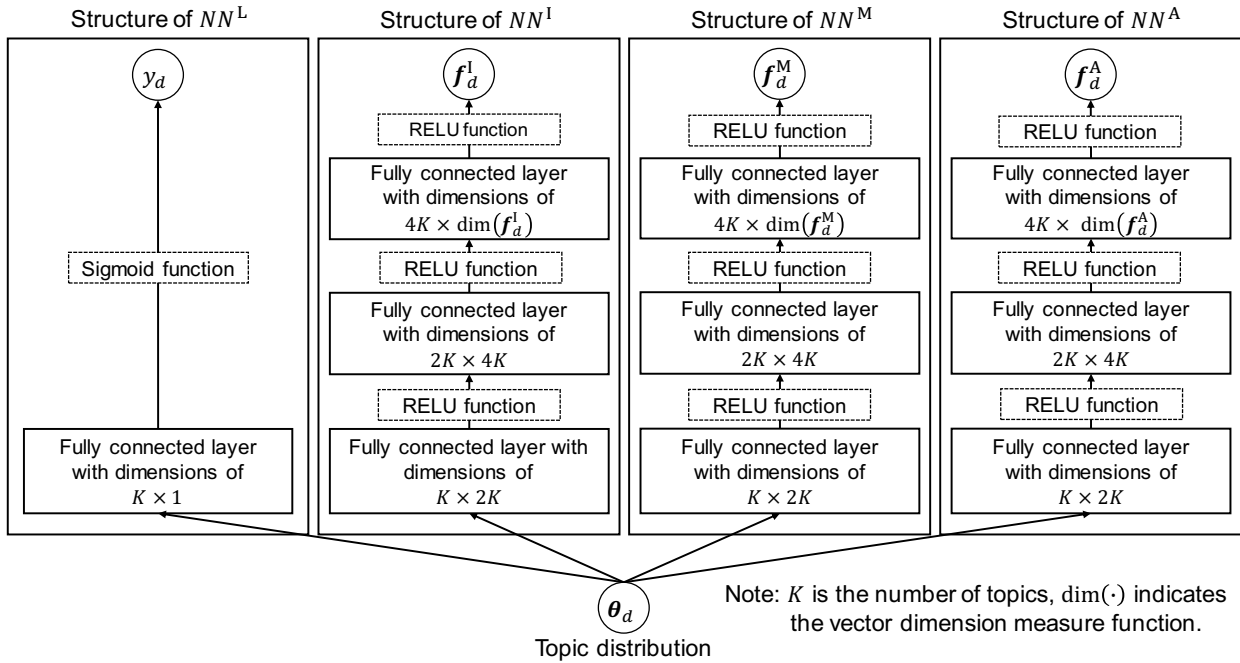
Zhu, Q., Z. Feng, and X. Li. 2018. "GraphBTM: Graph Enhanced Autoencoded Variational Inference for Biterm Topic Model," *Proceedings of the 2018 Conference on Empirical Methods in Natural Language Processing*pp. 4663-4672.

Zote, J. 2022. "The TikTok Algorithm Explained," *Sprout Social*May 2, .

Zulkarnain, N. Z., H. Basiron, and N. Abdullah. 2020, "Writing Style and Word Usage in Detecting Depression in Social Media: A Review," *Journal of Theoretical and Applied Information Technology* (98:1), pp. 124-135.

## APPENDICES

### 1. Architectural Details of the Neural Networks in the Generative Process



### 2. Proof of the Theorem

Without loss of generality, we show the proof for  $\tilde{\theta}_d^1$ . We denote  $\mathbf{I}_d^{-1}$  as the vector that does not include the first element, while other elements are the same as  $\mathbf{I}_d$ . Similar notations apply to  $\mathbf{h}_d^{-1}$ .

As  $\tilde{\theta}_d$  is normalized where  $k$ -th element  $\tilde{\theta}_d^k$  is  $\frac{h_d^k}{\sum_{i=1}^K h_d^i \cdot I_d^i}$  if  $I_d^k = 1$  and is 0 if  $I_d^k = 0$ . We denote

this normalization process as  $\tilde{\theta}_d = \text{Normalize}(\mathbf{h}_d \circ \mathbf{I}_d)$ . Hence, each  $\tilde{\theta}_d$  corresponds to a  $\mathbf{I}_d$  and

vice versa. Hence, we have  $p(\tilde{\boldsymbol{\theta}}_d | \mathbf{h}_d) = p(\mathbf{I}_d | \mathbf{h}_d)$ .

$$\begin{aligned}
\mathbb{E}_{\tilde{\boldsymbol{\theta}}_d \sim p(\tilde{\boldsymbol{\theta}}_d | \mathbf{h}_d)} \tilde{\theta}_d^1 &= \mathbb{E}_{\mathbf{I}_d \sim p(\mathbf{I}_d | \mathbf{h}_d)} \tilde{\theta}_d^1 \\
&= h_d^1 \cdot \mathbb{E}_{\mathbf{I}_d^{-1} \sim p(\mathbf{I}_d^{-1} | \mathbf{h}_d^{-1}, I_d^1 = 1)} h_d^1 \frac{1}{h_d^1 + \sum_{k=1, k \neq 1}^K (h_d^k \cdot I_d^k)} + (1 - h_d^1) \cdot 0 \\
&= (h_d^1)^2 \cdot \mathbb{E}_{\mathbf{I}_d^{-1} \sim p(\mathbf{I}_d^{-1} | \mathbf{h}_d^{-1}, I_d^1 = 1)} \frac{1}{h_d^1 + \sum_{k=1, k \neq 1}^K (h_d^k \cdot I_d^k)} \\
&\geq (h_d^1)^2 \frac{1}{\mathbb{E}_{\mathbf{I}_d^{-1} \sim p(\mathbf{I}_d^{-1} | \mathbf{h}_d^{-1}, I_d^1 = 1)} [h_d^1 + \sum_{k=1, k \neq 1}^K (h_d^k \cdot I_d^k)]} \\
&= (h_d^1)^2 \frac{1}{h_d^1 + \mathbb{E}_{\mathbf{I}_d^{-1} \sim p(\mathbf{I}_d^{-1} | \mathbf{h}_d^{-1}, I_d^1 = 1)} [\sum_{k=1, k \neq 1}^K (h_d^k \cdot I_d^k)]} \\
&= (h_d^1)^2 \frac{1}{h_d^1 + \sum_{k=1, k \neq 1}^K \mathbb{E}_{\mathbf{I}_d^{-1} \sim p(\mathbf{I}_d^{-1} | \mathbf{h}_d^{-1}, I_d^1 = 1)} (h_d^k \cdot I_d^k)} \\
&= (h_d^1)^2 \frac{1}{h_d^1 + \sum_{k=1, k \neq 1}^K \mathbb{E}_{I_d^k \sim p(I_d^k | h_d^k)} (h_d^k \cdot I_d^k)} \\
&= (h_d^1)^2 \frac{1}{h_d^1 + \sum_{k=1, k \neq 1}^K (h_d^k \cdot h_d^k + (1 - h_d^k) \cdot 0)} = (h_d^1)^2 \frac{1}{h_d^1 + \sum_{k=1, k \neq 1}^K (h_d^k)^2}
\end{aligned}$$

Note: As each variable  $I_d^k$  is independent,  $\mathbb{E}_{\mathbf{I}_d^{-1} \sim p(\mathbf{I}_d^{-1} | \mathbf{h}_d^{-1}, I_d^1 = 1)} (h_d^k \cdot I_d^k)$  can be reduced to

$\mathbb{E}_{I_d^k \sim p(I_d^k | h_d^k)} (h_d^k \cdot I_d^k)$ . Similar proof applies to each element of vector  $\tilde{\boldsymbol{\theta}}_d^{(n)}$ . Proof finished.

### 3. The Derivation of the KL Divergence

$$\begin{aligned}
\text{KL}^{\text{All}} &= \text{KL}\left(q_{\boldsymbol{\psi}}(\boldsymbol{\theta}, \tilde{\boldsymbol{\pi}}, \boldsymbol{\pi}, \boldsymbol{\phi}^S, \boldsymbol{\phi}^R, \tilde{\boldsymbol{\phi}}^R) \| p(\boldsymbol{\theta}, \tilde{\boldsymbol{\pi}}, \boldsymbol{\pi}, \boldsymbol{\phi}^S, \boldsymbol{\phi}^R, \tilde{\boldsymbol{\phi}}^R | \widetilde{W}, W, F^I, F^M, F^A, Y)\right) \\
&= \int q_{\boldsymbol{\psi}}(\boldsymbol{\theta}, \tilde{\boldsymbol{\pi}}, \boldsymbol{\pi}, \boldsymbol{\phi}^S, \boldsymbol{\phi}^R, \tilde{\boldsymbol{\phi}}^R) (\log q_{\boldsymbol{\psi}}(\boldsymbol{\theta}, \tilde{\boldsymbol{\pi}}, \boldsymbol{\pi}, \boldsymbol{\phi}^S, \boldsymbol{\phi}^R, \tilde{\boldsymbol{\phi}}^R) \\
&\quad - \log p(\boldsymbol{\theta}, \tilde{\boldsymbol{\pi}}, \boldsymbol{\pi}, \boldsymbol{\phi}^S, \boldsymbol{\phi}^R, \tilde{\boldsymbol{\phi}}^R | \widetilde{W}, W, F^I, F^M, F^A, Y)) d\boldsymbol{\theta} d\tilde{\boldsymbol{\pi}} d\boldsymbol{\pi} d\boldsymbol{\phi}^S d\boldsymbol{\phi}^R d\tilde{\boldsymbol{\phi}}^R \\
&= \mathbb{E}_{q_{\boldsymbol{\psi}}} [\log q_{\boldsymbol{\psi}}(\boldsymbol{\theta}, \tilde{\boldsymbol{\pi}}, \boldsymbol{\pi}, \boldsymbol{\phi}^S, \boldsymbol{\phi}^R, \tilde{\boldsymbol{\phi}}^R)] \\
&\quad - \mathbb{E}_{q_{\boldsymbol{\psi}}} [\log p(\boldsymbol{\theta}, \tilde{\boldsymbol{\pi}}, \boldsymbol{\pi}, \boldsymbol{\phi}^S, \boldsymbol{\phi}^R, \tilde{\boldsymbol{\phi}}^R | \widetilde{W}, W, F^I, F^M, F^A, Y)] \\
&= \mathbb{E}_{q_{\boldsymbol{\psi}}} [\log q_{\boldsymbol{\psi}}(\boldsymbol{\theta}, \tilde{\boldsymbol{\pi}}, \boldsymbol{\pi}, \boldsymbol{\phi}^S, \boldsymbol{\phi}^R, \tilde{\boldsymbol{\phi}}^R)] \\
&\quad - \mathbb{E}_{q_{\boldsymbol{\psi}}} \left[ \log \frac{p(\boldsymbol{\theta}, \tilde{\boldsymbol{\pi}}, \boldsymbol{\pi}, \boldsymbol{\phi}^S, \boldsymbol{\phi}^R, \tilde{\boldsymbol{\phi}}^R, \widetilde{W}, W, F^I, F^M, F^A, Y)}{p(\widetilde{W}, W, F^I, F^M, F^A, Y)} \right] \\
&= \mathbb{E}_{q_{\boldsymbol{\psi}}} [\log q_{\boldsymbol{\psi}}(\boldsymbol{\theta}, \tilde{\boldsymbol{\pi}}, \boldsymbol{\pi}, \boldsymbol{\phi}^S, \boldsymbol{\phi}^R, \tilde{\boldsymbol{\phi}}^R)] \\
&\quad - \mathbb{E}_{q_{\boldsymbol{\psi}}} [\log p(\boldsymbol{\theta}, \tilde{\boldsymbol{\pi}}, \boldsymbol{\pi}, \boldsymbol{\phi}^S, \boldsymbol{\phi}^R, \tilde{\boldsymbol{\phi}}^R, \widetilde{W}, W, F^I, F^M, F^A, Y) - \log p(\widetilde{W}, W, F^I, F^M, F^A, Y)] \\
&= \mathbb{E}_{q_{\boldsymbol{\psi}}} [\log q_{\boldsymbol{\psi}}(\boldsymbol{\theta}, \tilde{\boldsymbol{\pi}}, \boldsymbol{\pi}, \boldsymbol{\phi}^S, \boldsymbol{\phi}^R, \tilde{\boldsymbol{\phi}}^R) - \log p(\boldsymbol{\theta}, \tilde{\boldsymbol{\pi}}, \boldsymbol{\pi}, \boldsymbol{\phi}^S, \boldsymbol{\phi}^R, \tilde{\boldsymbol{\phi}}^R, \widetilde{W}, W, F^I, F^M, F^A, Y)] \\
&\quad + \mathbb{E}_{q_{\boldsymbol{\psi}}} [\log p(\widetilde{W}, W, F^I, F^M, F^A, Y)] \\
&= \mathbb{E}_{q_{\boldsymbol{\psi}}} [\log q_{\boldsymbol{\psi}}(\boldsymbol{\theta}, \tilde{\boldsymbol{\pi}}, \boldsymbol{\pi}, \boldsymbol{\phi}^S, \boldsymbol{\phi}^R, \tilde{\boldsymbol{\phi}}^R) - \log p(\boldsymbol{\theta}, \tilde{\boldsymbol{\pi}}, \boldsymbol{\pi}, \boldsymbol{\phi}^S, \boldsymbol{\phi}^R, \tilde{\boldsymbol{\phi}}^R, \widetilde{W}, W, F^I, F^M, F^A, Y)] \\
&\quad + \log p(\widetilde{W}, W, F^I, F^M, F^A, Y)
\end{aligned}$$

## 4. The Derivation of the ELBO

## 5. Architectural Details of the Inference Networks

